

**The protonmotive force and respiratory control:  
Building blocks of mitochondrial physiology  
Part 1.**

[http://www.mitoeagle.org/index.php/MitoEAGLE\\_preprint\\_2017-09-21](http://www.mitoeagle.org/index.php/MitoEAGLE_preprint_2017-09-21)

Preprint version 19 (2017-11-26)

**MitoEAGLE Network**

Corresponding author: Gnaiger E

Contributing co-authors

Ahn B, Alves MG, Amati F, Aral C, Arandarčikaitė O, Åsander Frostner E, Bailey DM, Bastos Sant'Anna Silva AC, Battino M, Beard DA, Ben-Shachar D, Bishop D, Breton S, Brown GC, Brown RA, Buettner GR, Calabria E, Cardoso LHD, Carvalho E, Casado Pinna M, Cervinkova Z, Chang SC, Chicco AJ, Coen PM, Collins JL, Crisóstomo L, Davis MS, Dias T, Distefano G, Doerrier C, Drahotka Z, Ehinger J, Elmer E, Endlicher R, Fell DA, Ferko M, Ferreira JCB, Filipovska A, Fisar Z, Fisher J, Garcia-Roves PM, Garcia-Souza LF, Genova ML, Gonzalo H, Goodpaster BH, Gorr TA, Grefte S, Han J, Harrison DK, Hellgren KT, Hernansanz P, Holland O, Hoppel CL, Houstek J, Iglesias-Gonzalez J, Irving BA, Iyer S, Jackson CB, Jansen-Dürr P, Jespersen NR, Jha RK, Kaambre T, Kane DA, Kappler L, Karabatsiakakis A, Keijer J, Keppner G, Komlodi T, Kopitar-Jerala N, Krako Jakovljevic N, Kuang J, Kucera O, Labieniec-Watala M, Lai N, Laner V, Larsen TS, Lee HK, Lemieux H, Lerfall J, Lucchinetti E, MacMillan-Crow LA, Makrecka-Kuka M, Meszaros AT, Michalak S, Moiso N, Molina AJA, Montaigne D, Moore AL, Moreira BP, Mracek T, Muntane J, Muntean DM, Murray AJ, Nedergaard J, Nemeč M, Newsom S, Nozickova K, O'Gorman D, Oliveira PF, Oliveira PJ, Orynbayeva Z, Pak YK, Palmeira CM, Patel HH, Pecina P, Pereira da Silva Grilo da Silva F, Pesta D, Petit PX, Pichaud N, Pirkmajer S, Porter RK, Pranger F, Prochownik EV, Puurand M, Radenkovic F, Reboredo P, Renner-Sattler K, Robinson MM, Rohlena J, Røslund GV, Rossiter HB, Rybacka-Mossakowska J, Salvadego D, Scatena R, Schartner M, Scheibye-Knudsen M, Schilling JM, Schlattner U, Schoenfeld P, Scott GR, Shabalina IG, Shevchuk I, Siewiera K, Singer D, Sobotka O, Spinazzi M, Stankova P, Stier A, Stocker R, Sumbalova Z, Suravajhala P, Tanaka M, Tandler B, Tepp K, Tomar D, Towheed A, Tretter L, Trivigno C, Tronstad KJ, Trougakos IP, Tyrrell DJ, Urban T, Velika B, Vendelin M, Vercesi AE, Victor VM, Villena JA, Wagner BA, Ward ML, Watala C, Wei YH, Wieckowski MR, Wohlwend M, Wolff J, Wuest RCI, Zaugg K, Zaugg M, Zorzano A

Supporting co-authors:

Bakker BM, Bernardi P, Boetker HE, Borsheim E, Borutaitė V, Bouitbir J, Calbet JA, Chaurasia B, Clementi E, Coker RH, Collin A, Das AM, De Palma C, Dubouchaud H, Duchon MR, Durham WJ, Dyrstad SE, Engin AB, Fornaro M, Gan Z, Garlid KD, Garten A, Gourlay CW, Granata C, Haas CB, Haavik J, Haendeler J, Hand SC, Hepple RT, Hickey AJ, Hoel F, Kainulainen H, Khamoui AV, Klingenspor M, Koopman WJH, Kowaltowski AJ, Krajcova A, Lenaz G, Malik A, Markova M, Mazat JP, Menze MA, Methner A, Muntanė J, Neuzil J, Oliveira MT, Pallotta ML, Parajuli N, Pettersen IKN, Porter C, Pulinilkunnit T, Ropelle ER, Salin K, Sandi C, Sazanov LA, Silber AM, Skolik R, Smenes BT, Soares FAA, Sokolova I, Sonkar VK, Swerdlow RH, Szabo I, Trifunovic A, Thyfault JP, Valentine JM, Vieyra A, Votion DM, Williams C

**Updates:**

[http://www.mitoeagle.org/index.php/MitoEAGLE\\_preprint\\_2017-09-21](http://www.mitoeagle.org/index.php/MitoEAGLE_preprint_2017-09-21)

Correspondence: Gnaiger E

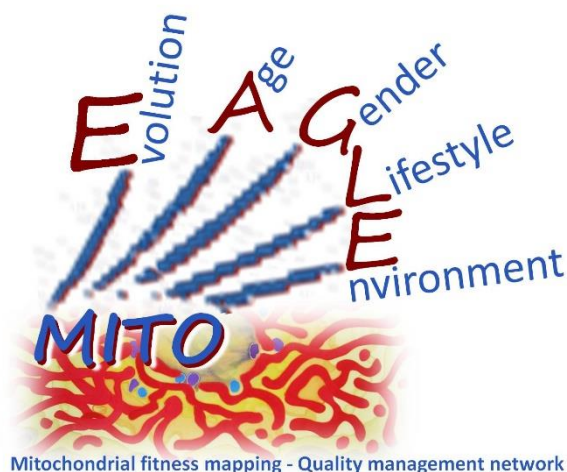
Department of Visceral, Transplant and Thoracic Surgery, D. Swarovski Research  
Laboratory, Medical University of Innsbruck, Innrain 66/4, A-6020 Innsbruck, Austria

Email: erich.gnaiger@i-med.ac.at

Tel: +43 512 566796, Fax: +43 512 566796 20

This manuscript on 'The protonmotive force and respiratory control' is a position statement in the frame of COST Action CA15203 MitoEAGLE. The list of co-authors evolved beyond **phase 1** in the **bottom-up** spirit of COST (phase 1 versions 1-44).

This is an open invitation to scientists and students to join as co-authors, to provide a balanced view on mitochondrial respiratory control, a fundamental introductory presentation of the concept of the protonmotive force, and a consensus statement on reporting data of mitochondrial respiration in terms of metabolic flows and fluxes.



**Phase 2:** MitoEAGLE preprint (Versions 01 – 15): We continue to invite comments and suggestions, particularly if you are an **early career investigator adding an open future-oriented perspective**, or an **established scientist providing a balanced historical basis**. Your critical input into the quality of the manuscript will be most welcome, improving our aims to be educational, general, consensus-oriented, and practically helpful for students working in mitochondrial respiratory physiology.

**Phase 3 (2017-11-11) Print version for MiP2017 and MitoEAGLE workshop in Hradec Kralove:**

» [http://www.mitoeagle.org/index.php/MiP2017\\_Hradec\\_Kralove\\_CZ](http://www.mitoeagle.org/index.php/MiP2017_Hradec_Kralove_CZ)

**Discussion of manuscript submission to a preprint server, such as BioRxiv; invite further opinion leaders:** To join as a co-author, please feel free to focus on a particular section in terms of direct input and references, contributing to the scope of the manuscript from the perspective of your expertise. Your comments will be largely posted on the discussion page of the MitoEAGLE preprint website.

If you prefer to submit comments in the format of a referee's evaluation rather than a contribution as a co-author, I will be glad to distribute your views to the updated list of co-authors for a balanced response. We would ask for your consent on this open bottom-up policy.

**Phase 4:** Journal submission. We plan a series of follow-up reports by the expanding MitoEAGLE Network, to increase the scope of recommendations on harmonization and facilitate global communication and collaboration. Further discussions: MitoEAGLE Working Group Meetings, various conferences (EBEC 2018 in Budapest).

I thank you in advance for your feedback.

With best wishes,

Erich Gnaiger

Chair Mitochondrial Physiology Society - <http://www.mitophysiology.org>

Chair COST Action MitoEAGLE - <http://www.mitoeagle.org>

103	<b>Contents</b>
104	<b>1. Introduction</b>
105	<b>2. Respiratory coupling states in mitochondrial preparations</b>
106	Mitochondrial preparations
107	2.1. <i>Three coupling states of mitochondrial preparations and residual oxygen consumption</i>
108	Coupling control states and respiratory capacities
109	Kinetic control
110	Phosphorylation, P <sub>o</sub>
111	LEAK, OXPHOS, ET, ROX
112	2.2. <i>Coupling states and respiratory rates</i>
113	2.3. <i>Classical terminology for isolated mitochondria</i>
114	States 1-5
115	<b>3. The protonmotive force and proton flux</b>
116	3.1. <i>Electric and chemical partial forces versus electrical and chemical units</i>
117	Faraday constant
118	Electric part of the protonmotive force
119	Chemical part of the protonmotive force
120	3.2. <i>Definitions</i>
121	Control and regulation
122	Respiratory control and response
123	Respiratory coupling control
124	Pathway control states
125	The steady-state
126	3.3. <i>Forces and fluxes in physics and thermodynamics</i>
127	Vectorial and scalar forces, and fluxes
128	Coupling
129	Coupled versus bound processes
130	<b>4. Normalization: fluxes and flows</b>
131	4.1. <i>Flux per chamber volume</i>
132	4.2. <i>System-specific and sample-specific normalization</i>
133	Extensive quantities
134	Size-specific quantities
135	Molar quantities
136	Flow per system, $I$
137	Size-specific flux, $J$
138	Sample concentration, $C_{mX}$
139	Mass-specific flux, $J_{mX,O_2}$
140	Number concentration, $C_{NX}$
141	Flow per sample entity, $I_{X,O_2}$
142	4.3. <i>Normalization for mitochondrial content</i>
143	Mitochondrial concentration, $C_{mte}$ , and mitochondrial markers
144	Mitochondria-specific flux, $J_{mte,O_2}$
145	4.4. <i>Evaluation of mitochondrial markers</i>
146	4.5. <i>Conversion: units and normalization</i>
147	4.6. <i>Conversion: oxygen, proton and ATP flux</i>
148	<b>5. Conclusions</b>
149	<b>6. References</b>
150	

151 **Abstract** Clarity of concept and consistency of nomenclature are key trademarks of a research  
 152 field. These trademarks facilitate effective transdisciplinary communication, education, and  
 153 ultimately further discovery. As the knowledge base and importance of mitochondrial  
 154 physiology to human health expand, the necessity for harmonizing nomenclature concerning  
 155 mitochondrial respiratory states and rates has become increasingly apparent. Peter Mitchell's  
 156 chemiosmotic theory establishes the links between electrical and chemical components of  
 157 energy transformation and coupling in oxidative phosphorylation. This unifying concept of the  
 158 protonmotive force provides the framework for developing a consistent nomenclature for  
 159 mitochondrial physiology and bioenergetics. Herein, we follow IUPAC guidelines on general  
 160 terms of physical chemistry, extended by the concepts of open systems and irreversible  
 161 thermodynamics. We align the nomenclature of classical bioenergetics on respiratory states  
 162 with a concept-driven constructive terminology to address the meaning of each respiratory state.  
 163 Furthermore, we suggest uniform standards for the evaluation of respiratory states that will  
 164 ultimately support the development of databases of mitochondrial respiratory function in  
 165 species, tissues and cells studied under diverse physiological and experimental conditions. In  
 166 this position statement, in the frame of COST Action MitoEAGLE, we endeavour to provide a  
 167 balanced view on mitochondrial respiratory control, a fundamental introductory presentation of  
 168 the concept of the protonmotive force, and a critical discussion on reporting data of  
 169 mitochondrial respiration in terms of metabolic flows and fluxes.

170  
 171 *Keywords:* Mitochondrial respiratory control, coupling control, mitochondrial  
 172 preparations, protonmotive force, chemiosmotic theory, oxidative phosphorylation, OXPHOS,  
 173 efficiency, electron transfer, ET; proton leak, LEAK, residual oxygen consumption, ROX, State  
 174 2, State 3, State 4, normalization, flow, flux  
 175

176 **Box 1:**

177 **In brief:**  
 178 **mitochondria**  
 179 **and Bioblasts**

- Does the public expect biologists to understand Darwin's theory of evolution?
- Do students expect that researchers of bioenergetics can explain Mitchell's theory of chemiosmotic energy transformation?

182 **Mitochondria** were described by Richard Altmann (1894) as 'bioblasts', which include not  
 183 only the mitochondria as presently defined, but also symbiotic and free-living bacteria. The  
 184 word 'mitochondrium' (Greek mitos: thread; chondros: granule) was introduced by Carl Benda  
 185 (1898). Mitochondria are the oxygen-consuming electrochemical generators which evolved  
 186 from endosymbiotic bacteria (Margulis 1970; Lane 2005).

187 We now recognize mitochondria as dynamic organelles with a double membrane that are  
 188 contained within eukaryotic cells. The mitochondrial inner membrane (mtIM) shows dynamic  
 189 tubular to disk-shaped cristae that separate the mitochondrial matrix, *i.e.* the internal  
 190 mitochondrial compartment, and the intermembrane space; the latter being enclosed by the  
 191 mitochondrial outer membrane (mtOM). Mitochondria are the structural and functional  
 192 elemental units of cell respiration. Cell respiration is the consumption of oxygen by electron  
 193 transfer coupled to electrochemical proton translocation across the mtIM. In the process of  
 194 oxidative phosphorylation (OXPHOS), the reduction of O<sub>2</sub> is electrochemically coupled to the  
 195 transformation of energy in the form of adenosine triphosphate (ATP; Mitchell 1961, 2011).  
 196 These powerhouses of the cell contain the machinery of the OXPHOS-pathway, including  
 197 transmembrane respiratory complexes (*i.e.* proton pumps with FMN, Fe-S and cytochrome *b*,  
 198 *c*, *aa*<sub>3</sub> redox systems); alternative dehydrogenases and oxidases; the coenzyme ubiquinone (Q);  
 199 ATP synthase; the enzymes of the tricarboxylic acid cycle and the fatty acid oxidation enzymes;  
 200 transporters of ions, metabolites and co-factors; and mitochondrial kinases related to energy  
 201 transfer pathways. The mitochondrial proteome comprises over 1,200 proteins  
 202 (MITOCARTA), mostly encoded by nuclear DNA (nDNA), with a variety of functions, many



203 of which are relatively well known (e.g. apoptosis-regulating proteins), while others are still  
 204 under investigation, or need to be identified (e.g. alanine transporter).

205 Mitochondria typically maintain several copies of their own genome (hundred to  
 206 thousands per cell; Cummins 1998), which is almost exclusively maternally inherited (White *et*  
 207 *al.* 2008) and known as mitochondrial DNA (mtDNA). One exception to strictly maternal  
 208 inheritance in animals is found in bivalves (Breton *et al.* 2007). mtDNA is 16.5 kB in length,  
 209 contains 13 protein-coding genes for subunits of the transmembrane respiratory Complexes CI,  
 210 CIII, CIV and ATP synthase, and also encodes 22 tRNAs and the mitochondrial 16S and 12S  
 211 rRNA. The mitochondrial genome is both regulated and supplemented by nuclear-encoded  
 212 mitochondrial targeted proteins. Evidence has accumulated that additional gene content is  
 213 encoded in the mitochondrial genome, e.g. microRNAs, piRNA, smithRNAs, repeat associated  
 214 RNA, and even additional proteins (Duarte *et al.* 2014; Lee *et al.* 2015; Cobb *et al.* 2016).

215 The mtIM contains the non-bilayer phospholipid cardiolipin, which is not present in any  
 216 other eukaryotic cellular membrane. Cardiolipin promotes the formation of respiratory  
 217 supercomplexes, which are supramolecular assemblies based upon specific, though dynamic,  
 218 interactions between individual respiratory complexes (Greggio *et al.* 2017; Lenaz *et al.* 2017).  
 219 Membrane fluidity is an important parameter influencing functional properties of proteins  
 220 incorporated in the membranes (Waczulikova *et al.* 2007). There is a constant crosstalk between  
 221 mitochondria and the other cellular components, maintaining cellular mitostasis through  
 222 regulation at both the transcriptional and post-translational level, and through cell signalling  
 223 including proteostatic (e.g. the ubiquitin-proteasome and autophagy-lysosome pathways) and  
 224 genome stability modules throughout the cell cycle or even cell death, contributing to  
 225 homeostatic regulation in response to varying energy demands and stress (Quiros *et al.* 2016).  
 226 In addition to mitochondrial movement along the microtubules, mitochondrial morphology can  
 227 change in response to the energy requirements of the cell via processes known as fusion and  
 228 fission, through which mitochondria can communicate within a network, and in response to  
 229 intracellular stress factors causing swelling and ultimately permeability transition.

230 Mitochondrial dysfunction is associated with a wide variety of genetic and degenerative  
 231 diseases. Robust mitochondrial function is supported by physical exercise and caloric balance,  
 232 and is central for sustained metabolic health throughout life. Therefore, a more consistent  
 233 presentation of mitochondrial physiology will improve our understanding of the etiology of  
 234 disease, the diagnostic repertoire of mitochondrial medicine, with a focus on protective  
 235 medicine, lifestyle and healthy aging.

236 Abbreviation: mt, as generally used in mtDNA. Mitochondrion is singular and  
 237 mitochondria is plural.

238 *‘For the physiologist, mitochondria afforded the first opportunity for an experimental*  
 239 *approach to structure-function relationships, in particular those involved in active transport,*  
 240 *vectorial metabolism, and metabolic control mechanisms on a subcellular level’* (Ernster and  
 241 Schatz 1981).

242

## 243 1. Introduction

244

245 Mitochondria are the powerhouses of the cell with numerous physiological, molecular,  
 246 and genetic functions (**Box 1**). Every study of mitochondrial function and disease is faced with  
 247 **E**volution, **A**ge, **G**ender and sex, **L**ifestyle, and **E**nvironment (EAGLE) as essential background  
 248 conditions intrinsic to the individual patient or subject, cohort, species, tissue and to some extent  
 249 even cell line. As a large and highly coordinated group of laboratories and researchers, the  
 250 mission of the global MitoEAGLE Network is to generate the necessary scale, type, and quality  
 251 of consistent data sets and conditions to address this intrinsic complexity. Harmonization of  
 252 experimental protocols and implementation of a quality control and data management system  
 253 is required to interrelate results gathered across a spectrum of studies and to generate a

254 rigorously monitored database focused on mitochondrial respiratory function. In this way,  
255 researchers within the same and across different disciplines will be positioned to compare their  
256 findings to an agreed upon set of clearly defined and accepted international standards.

257 Reliability and comparability of quantitative results depend on the accuracy of  
258 measurements under strictly-defined conditions. A conceptually defined framework is also  
259 required to warrant meaningful interpretation and comparability of experimental outcomes  
260 carried out by research groups at different institutes. With an emphasis on quality of research,  
261 collected data can be useful far beyond the specific question of a particular experiment.  
262 Enabling meta-analytic studies is the most economic way of providing robust answers to  
263 biological questions (Cooper *et al.* 2009). Vague or ambiguous jargon can lead to confusion  
264 and may relegate valuable signals to wasteful noise. For this reason, measured values must be  
265 expressed in standardized units for each parameter used to define mitochondrial respiratory  
266 function. Standardization of nomenclature and definition of technical terms is essential to  
267 improve the awareness of the intricate meaning of a divergent scientific vocabulary, for  
268 documentation and integration into databases in general, and quantitative modelling in  
269 particular (Beard 2005). The focus on the protonmotive force, coupling states, and fluxes  
270 through metabolic pathways of aerobic energy transformation in mitochondrial preparations is  
271 a first step in the attempt to generate a harmonized and conceptually-oriented nomenclature in  
272 bioenergetics and mitochondrial physiology. Coupling states of intact cells and respiratory  
273 control by fuel substrates and specific inhibitors of respiratory enzymes will be reviewed in  
274 subsequent communications.

275

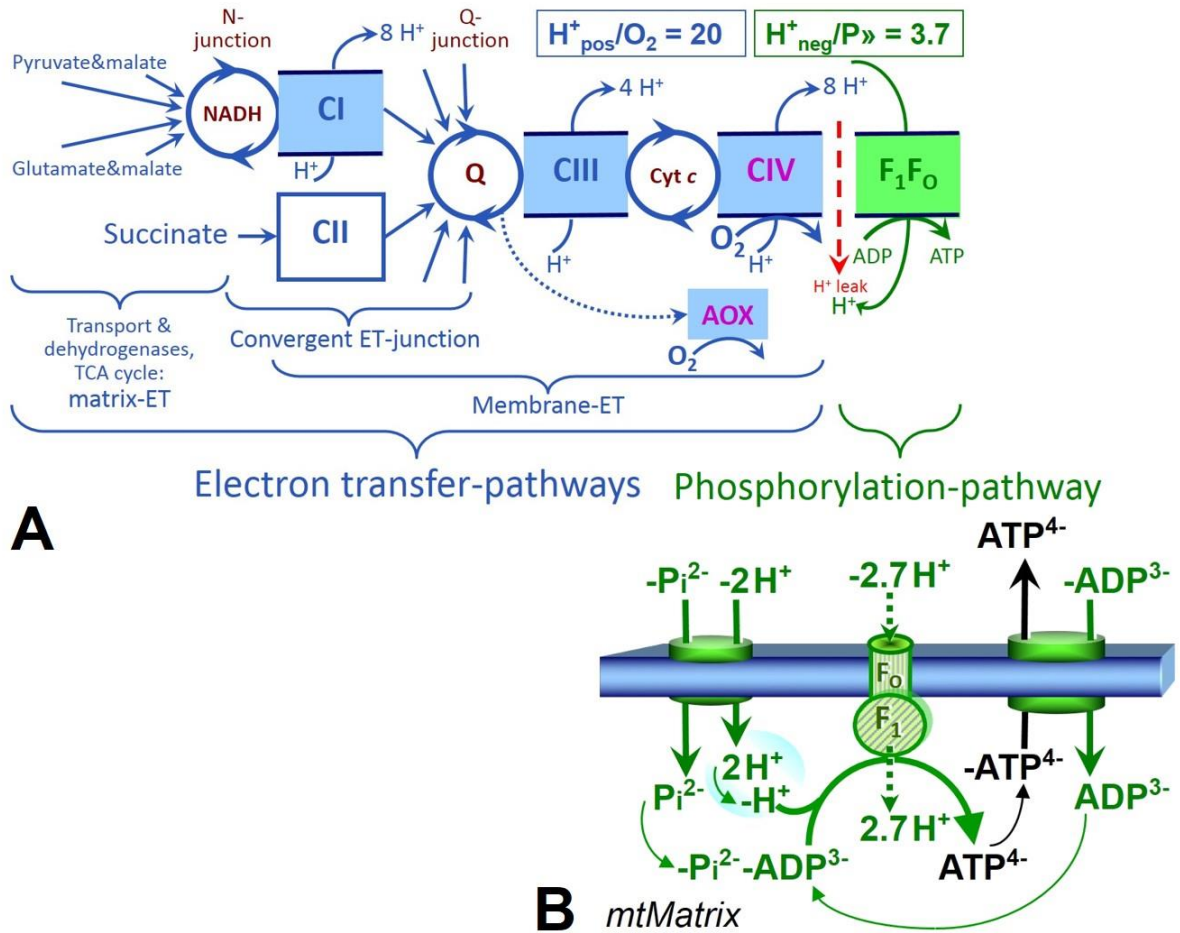
## 276 **2. Respiratory coupling states in mitochondrial preparations**

277 *‘Every professional group develops its own technical jargon for talking about*  
278 *matters of critical concern ... People who know a word can share that idea with*  
279 *other members of their group, and a shared vocabulary is part of the glue that holds*  
280 *people together and allows them to create a shared culture’ (Miller 1991).*

281

282 **Mitochondrial preparations** are defined as either isolated mitochondria, or tissue and  
283 cellular preparations in which the barrier function of the plasma membrane is disrupted. The  
284 plasma membrane separates the cytosol, nucleus, and organelles (the intracellular  
285 compartment) from the environment of the cell. The plasma membrane consists of a lipid  
286 bilayer, embedded proteins, and attached organic molecules that collectively control the  
287 selective permeability of ions, organic molecules, and particles across the cell boundary. The  
288 intact plasma membrane, therefore, prevents the passage of many water-soluble mitochondrial  
289 substrates, such as succinate or adenosine diphosphate (ADP), that are required for the analysis  
290 of respiratory capacity at kinetically-saturating concentrations, thus limiting the scope of  
291 investigations into mitochondrial respiratory function in intact cells. The cholesterol content of  
292 the plasma membrane is high compared to mitochondrial membranes. Therefore, mild  
293 detergents, such as digitonin and saponin, can be applied to selectively permeabilize the plasma  
294 membrane by interaction with cholesterol and allow free exchange of cytosolic components  
295 with ions and organic molecules of the immediate cell environment, while maintaining the  
296 integrity and localization of organelles, cytoskeleton, and the nucleus. Application of optimum  
297 concentrations of permeabilization agents (mild detergents or toxins) leads to the complete loss  
298 of cell viability, tested by nuclear staining and washout of cytosolic marker enzymes such as  
299 lactate dehydrogenase, while mitochondrial function remains intact. The respiration rate of  
300 isolated mitochondria remains unaltered after the addition of low concentrations of digitonin and  
301 saponin. In addition to mechanical permeabilization during homogenization of fresh tissue,  
302 permeabilization agents may be applied to ensure permeabilization of all cells. Crude  
303 homogenate and cells permeabilized in the respiration chamber contain all components of the  
304 cell at highly diluted concentrations. All mitochondria are retained in chemically-permeabilized

305 mitochondrial preparations and crude tissue homogenates. In the preparation of isolated  
 306 mitochondria, the cells or tissues are homogenized, and the mitochondria are separated from  
 307 other cell fractions and purified by differential centrifugation, entailing the loss of a fraction of  
 308 mitochondria. Typical mitochondrial yields range from 30% to 80%. Maximization of the  
 309 purity of isolated mitochondria may compromise not only the mitochondrial yield but also the  
 310 structural and functional integrity. Therefore, protocols for isolation of mitochondria need to be  
 311 optimized according to the relevant questions addressed in a study. The mitochondrial yield and  
 312 experimental criteria for evaluation of purity versus integrity should be reported. The term  
 313 mitochondrial preparation does not include further fractionation of mitochondrial components,  
 314 as well as submitochondrial particles.  
 315



316  
 317 **Fig. 1. The oxidative phosphorylation-pathway, OXPHOS-pathway.** (A) Electron transfer,  
 318 ET, coupled to phosphorylation. ET-pathways converge at the N- and Q-junction, as shown for  
 319 the NADH- and succinate-pathway; additional arrows indicate electron entry into the Q-  
 320 junction through electron transferring flavoprotein, glycerophosphate dehydrogenase, dihydro-  
 321 orotate dehydrogenase, choline dehydrogenase, and sulfide-ubiquinone oxidoreductase. The  
 322 branched pathway of oxygen consumption by alternative quinol oxidase (AOX) is indicated by  
 323 the dotted arrow. The  $H^+_{pos}/O_2$  ratio is the outward proton flux from the matrix space to the  
 324 positively (pos) charged compartment, divided by catabolic O<sub>2</sub> flux in the NADH-pathway. The  
 325  $H^+_{neg}/P \gg$  ratio is the inward proton flux from the inter-membrane space to the negatively (neg)  
 326 charged matrix space, divided by the flux of phosphorylation of ADP to ATP. Due to ion leaks  
 327 and proton slip these are not fixed stoichiometries. (B) Phosphorylation-pathway catalyzed by  
 328 the F<sub>1</sub>F<sub>0</sub> ATP synthase, adenine nucleotide translocase, and inorganic phosphate transporter.  
 329 The  $H^+_{neg}/P \gg$  stoichiometry is the sum of the coupling stoichiometry in the ATP synthase  
 330 reaction (-2.7 H<sup>+</sup> from the intermembrane space, 2.7 H<sup>+</sup> to the matrix) and the proton balance

331 in the translocation of  $\text{ADP}^{2-}$ ,  $\text{ATP}^{3-}$  and  $\text{P}_i^{2-}$ . See Eqs. 5 and 6 for further explanation. Modified  
 332 from (A) Lemieux *et al.* (2017) and (B) Gnaiger (2014).

333

### 334 2.1. Three coupling states of mitochondrial preparations and residual oxygen consumption

335

336 **Respiratory capacities in coupling control states:** To extend the classical nomenclature  
 337 on mitochondrial coupling states (Section 2.4) by a concept-driven terminology that  
 338 incorporates explicit information on the nature of the respiratory states, the terminology must  
 339 be general and not restricted to any particular experimental protocol or mitochondrial  
 340 preparation (Gnaiger 2009). We focus primarily on the conceptual ‘why’, along with  
 341 clarification of the experimental ‘how’. In the following section, the concept-driven  
 342 terminology is explained and coupling states are defined. We define respiratory capacities,  
 343 comparable to channel capacity in information theory (Schneider 2006), as the upper bound of  
 344 the rate of respiration measured in defined coupling control states and electron transfer-pathway  
 345 (ET-pathway) states. To provide a diagnostic reference for respiratory capacities of core energy  
 346 metabolism, the capacity of *oxidative phosphorylation*, OXPHOS, is measured at kinetically-  
 347 saturating concentrations of ADP and inorganic phosphate,  $\text{P}_i$ . The *oxidative* ET-capacity  
 348 reveals the limitation of OXPHOS-capacity mediated by the *phosphorylation*-pathway. The  
 349 ET- and phosphorylation-pathways comprise coupled segments of the OXPHOS-pathway. ET-  
 350 capacity is measured as noncoupled respiration by application of *external uncouplers*. The  
 351 contribution of *intrinsically uncoupled* oxygen consumption is most easily studied in the  
 352 absence of ADP, *i.e.* by not stimulating phosphorylation, or by inhibition of the  
 353 phosphorylation-pathway. The corresponding states are collectively classified as LEAK-states,  
 354 when oxygen consumption compensates mainly for ion leaks including the proton leak (**Table**  
 355 **1**). Different coupling states are induced by: (1) adding cation chelators such as EGTA, binding  
 356 free  $\text{Ca}^{2+}$  and thus limiting cation cycling; (2) adding ADP or  $\text{P}_i$ ; (3) inhibiting the  
 357 phosphorylation-pathway; and (4) uncoupler titrations, while maintaining a defined ET-  
 358 pathway state with constant fuel substrates and inhibitors of specific branches of the ET-  
 359 pathway (**Fig. 1**).

360 **Kinetic control:** Coupling control states are established in the study of mitochondrial  
 361 preparations to obtain reference values for various output variables. Physiological conditions *in*  
 362 *vivo* deviate from these experimentally obtained states. Since kinetically-saturating  
 363 concentrations, *e.g.* of ADP or oxygen, may not apply to physiological intracellular conditions,  
 364 relevant information is obtained in studies of kinetic responses to conditions intermediate  
 365 between the LEAK state at zero [ADP] and the OXPHOS-state at saturating [ADP], or of  
 366 respiratory capacities in the range between kinetically-saturating  $[\text{O}_2]$  and anoxia (Gnaiger  
 367 2001).

368 **Specification of dose of biochemical additions:** Nominal concentrations of substrates,  
 369 uncouplers, inhibitors, and other biochemical reagents titrated to dissect mitochondrial function  
 370 are usually reported as initial amount of substance concentration  $[\text{mol}\cdot\text{L}^{-1}]$  in the incubation  
 371 medium. When aiming at the measurement of kinetically saturated processes such as OXPHOS  
 372 capacities, the concentrations for substrates can be chosen in light of the  $K_m$ . In the case of  
 373 hyperbolic kinetics, only 80% of maximum respiratory capacity is obtained at a substrate  
 374 concentration of four times the  $K_m$ , whereas substrate concentrations of 5, 9, 19 and 49 times  
 375 the  $K_m$  are theoretically required for reaching 83.3%, 90%, 95% or 98% of the maximal rate  
 376 (Gnaiger 2001). Other reagents are chosen to inhibit or alter some process. The amount of these  
 377 tools in an experimental incubation is selected to maximize effect, yet not lead to unacceptable  
 378 off-target consequences that would adversely affect the data being sought. Specifying the  
 379 amount of substance in an incubation as nominal concentration in the aqueous incubation  
 380 medium can be ambiguous (Doskey *et al.* 2015), particularly when lipid-soluble substances  
 381 (oligomycin; uncouplers, permeabilization agents) or cations ( $\text{TPP}^+$ ; fluorescent dyes such as



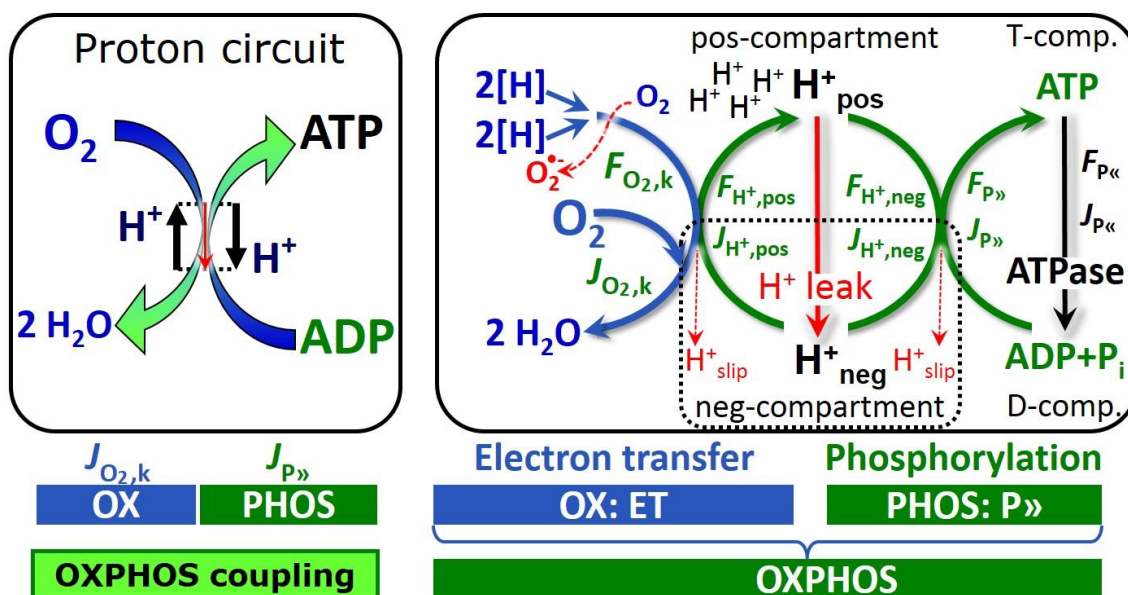
382 safranin, TMRM) are applied which accumulate in biological membranes or in the  
 383 mitochondrial matrix, respectively. For example, a dose of digitonin of  $8 \text{ fmol}\cdot\text{cell}^{-1}$  ( $10 \mu\text{g}\cdot 10^{-6}$   
 384 cells) is optimal for permeabilization of endothelial cells, and the concentration in the  
 385 incubation medium has to be adjusted according to the cell density applied (Doerrier *et al.*  
 386 2017). Generally, dose/exposure can be specified per unit of biological sample, *i.e.* (nominal  
 387 moles of xenobiotic)/(number of cells) [ $\text{mol}\cdot\text{cell}^{-1}$ ] or, as appropriate, per mass of biological  
 388 sample [ $\text{mol}\cdot\text{kg}^{-1}$ ]. This approach to specification of dose/exposure provides a scalable  
 389 parameter that can be used to design experiments, help interpret a wide variety of experimental  
 390 results, and provide absolute information that allows researchers worldwide to make the most  
 391 use of published data (Doskey *et al.* 2015).

392  
 393 **Table 1. Coupling states and residual oxygen consumption in mitochondrial**  
 394 **preparations in relation to respiration- and phosphorylation-rate,  $J_{\text{O}_2,\text{k}}$  and  $J_{\text{P}\gg}$ ,**  
 395 **and protonmotive force,  $F_{\text{H}^+,\text{pos}}$ .** Coupling states are established at kinetically-  
 396 saturating concentrations of fuel substrates and  $\text{O}_2$ .

State	$J_{\text{O}_2,\text{k}}$	$J_{\text{P}\gg}$	$F_{\text{H}^+,\text{pos}}$	Inducing factors	Limiting factors
LEAK	$L$ ; low, proton leak-dependent respiration	0	max.	Proton leak, slip, and cation cycling	$J_{\text{P}\gg} = 0$ : (1) without ADP, $L_N$ ; (2) max. ATP/ADP ratio, $L_T$ ; or (3) inhibition of the phosphorylation-pathway, $L_{\text{Omy}}$
OXPHOS	$P$ ; high, ADP-stimulated respiration	max.	high	Kinetically-saturating [ADP] and [ $\text{P}_i$ ]	$J_{\text{P}\gg}$ by phosphorylation-pathway; or $J_{\text{O}_2,\text{k}}$ by ET-capacity
ET	$E$ ; max., noncoupled respiration	0	low	Optimal external uncoupler concentration for max. oxygen flux	$J_{\text{O}_2,\text{k}}$ by ET-capacity
ROX	$R_{\text{ox}}$ ; min., residual $\text{O}_2$ consumption	0	0	$J_{\text{O}_2,\text{Rox}}$ in non-ET-pathway oxidation reactions	Full inhibition of ET-pathway; or absence of fuel substrates

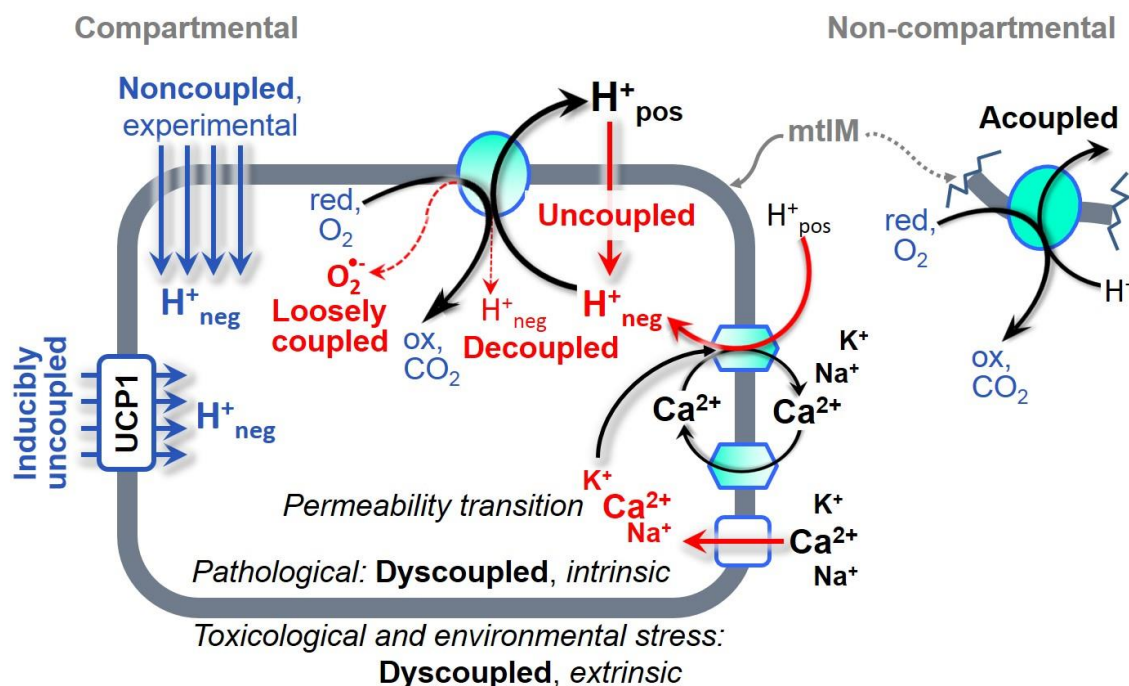
397  
 398 **Phosphorylation,  $\text{P}\gg$ :** *Phosphorylation* in the context of OXPHOS is defined as  
 399 phosphorylation of ADP to ATP. On the other hand, the term phosphorylation is used generally  
 400 in many different contexts, *e.g.* protein phosphorylation. This justifies consideration of a  
 401 symbol more discriminating and specific than P as used in the P/O ratio (phosphate to atomic  
 402 oxygen ratio;  $\text{O} = 0.5 \text{ O}_2$ ), where P indicates phosphorylation of ADP to ATP or GDP to GTP.  
 403 We propose the symbol  $\text{P}\gg$  for the endergonic direction of phosphorylation  $\text{ADP}\rightarrow\text{ATP}$ , and  
 404 likewise the symbol  $\text{P}\ll$  for the corresponding exergonic hydrolysis  $\text{ATP}\rightarrow\text{ADP}$  (**Fig. 2; Box**  
 405 **3**).  $J_{\text{P}\gg}/J_{\text{O}_2,\text{k}}$  ( $\text{P}\gg/\text{O}_2$ ) is two times the ‘P/O’ ratio of classical bioenergetics. ATP synthase is  
 406 proton pump of the phosphorylation-pathway (**Fig. 1B**).  $\text{P}\gg$  may also involve substrate-level  
 407 phosphorylation as part of the tricarboxylic acid cycle (succinyl-CoA ligase) and  
 408 phosphorylation of ADP catalyzed by phosphoenolpyruvate carboxykinase, adenylate kinase,  
 409 creatine kinase, hexokinase and nucleoside diphosphate kinase. Kinase cycles are involved in  
 410 intracellular energy transfer and signal transduction for regulation of energy flux. In isolated  
 411 mammalian mitochondria ATP production catalyzed by adenylate kinase,  $2\text{ADP} \leftrightarrow \text{ATP} +$   
 412 AMP, proceeds without fuel substrates in the presence of ADP (Komlódi and Tretter 2017).

413



414 **Fig. 2. The proton circuit and coupling in oxidative phosphorylation (OXPHOS).** Oxygen  
 415 flux,  $J_{O_2,k}$ , through the catabolic ET-pathway, k, is coupled to flux through the phosphorylation-  
 416 pathway of ADP to ATP,  $J_{P\gg}$ , by the proton pumps of the ET-pathway, driving the outward  
 417 proton flux,  $J_{H^+,pos}$ , and generating the output protonmotive force,  $F_{H^+,pos}$ . ATP synthase is  
 418 coupled to inward proton flux,  $J_{H^+,neg}$ , to phosphorylate  $ADP+P_i$  to ATP, driven by the input  
 419 protonmotive force,  $F_{H^+,neg} = -F_{H^+,pos}$ .  $2[H]$  indicates the reduced hydrogen equivalents of fuel  
 420 substrates that provide the chemical input force,  $F_{O_2,k}$  [kJ/mol  $O_2$ ], of the catabolic reaction k  
 421 with oxygen (Gibbs energy of reaction per mole  $O_2$  consumed in reaction k), typically in the  
 422 range of -460 to -480 kJ/mol (1.2 V). The output force is given by the phosphorylation potential  
 423 difference (ADP phosphorylated to ATP),  $F_{P\gg}$ , which varies *in vivo* ranging from about 48 to  
 424 62 kJ/mol under physiological conditions (Gnaiger 1993a). Fluxes,  $J_B$ , and forces,  $F_B$ , are  
 425 expressed in either chemical units, [ $mol \cdot s^{-1} \cdot m^{-3}$ ] and [ $J \cdot mol^{-1}$ ] respectively, or electrical units,  
 426 [ $C \cdot s^{-1} \cdot m^{-3}$ ] and [ $V = J \cdot C^{-1}$ ] respectively. Fluxes are expressed per volume,  $V$  [ $m^3$ ], of the system.  
 427 The system defined by the boundaries (full black line) is not a black box, but is analysed as a  
 428 compartmental system. The negative compartment (neg-compartment, enclosed by the dotted  
 429 line) is the matrix space, separated by the mtIM from the positive compartment (pos-  
 430 compartment).  $ADP+P_i$  and  $ATP$  are the substrate- and product-compartments (scalar ADP and  
 431 ATP compartments, D-comp. and T-comp.), respectively. Chemical potentials of all substrates  
 432 and products involved in the scalar reactions are measured in the pos-compartment for  
 433 calculation of the scalar forces  $F_{O_2,k}$  and  $F_{P\gg} = -F_{P\ll}$  (**Box 2**). Modified from Gnaiger (2014).  
 434  
 435

436 **Uncoupling:** The effective  $P\gg/O_2$  ratio is diminished by uncoupling, which is a general  
 437 term comprising diverse mechanisms (**Fig. 3**): (1) The proton leak across the mtIM from low  
 438 pH in the positively charged compartment to high pH in the negatively charged compartment;  
 439 (2) cycling of other cations, strongly stimulated by permeability transition; (3) proton slip in  
 440 the proton pumps when protons are effectively not pumped; (4) loss of compartmental integrity;  
 441 and (5) electron leak in the univalent reduction of oxygen ( $O_2$ ; dioxygen) to superoxide anion  
 442 radical ( $O_2^{\cdot-}$ ).  
 443



444  
 445 **Fig 3. Mechanisms of respiratory uncoupling.** An intact mitochondrial inner membrane,  
 446 mtIM, is the requirement of vectorial, compartmental coupling. Acoupled respiration is the  
 447 consequence of structural disruption with catalytic activity of non-compartmental  
 448 mitochondrial fragments. Inducibly uncoupled (activation of UCP1) and experimentally  
 449 noncoupled respiration (titration of protonophores) stimulate respiration to maximum oxygen  
 450 flux of ET-capacity. Uncoupled, decoupled, and loosely coupled respiration are components of  
 451 intrinsic LEAK respiration. Pathological dysfunction may affect all types of uncoupling,  
 452 including permeability transition, causing intrinsically dyscoupled respiration. Similarly,  
 453 toxicological and environmental stress factors can cause extrinsically dyscoupled respiration.


454  
 455 **LEAK-state (Fig. 4):** The  
 456 LEAK-state is defined as a state  
 457 of mitochondrial respiration  
 458 when  $O_2$  flux mainly  
 459 compensates for ion leaks in the  
 460 absence of ATP synthesis, at  
 461 kinetically-saturating  
 462 concentrations of  $O_2$  and  
 463 respiratory fuel substrates.  
 464 LEAK-respiration is measured to  
 465 obtain an estimate of *intrinsic*  
 466 *uncoupling* without addition of  
 467 any experimental uncoupler: (1)  
 468 in the absence of adenylates; (2)  
 469 after depletion of ADP at  
 470 maximum ATP/ADP ratio; or (3)  
 471 after inhibition of the  
 472 phosphorylation-pathway by  
 473 inhibitors of ATP synthase, such as oligomycin, or adenine nucleotide translocase, such as  
 474 carboxyatractyloside. It is important to consider adjustment of the nominal concentration of  
 475 these inhibitors to the density of biological sample applied, to minimize or avoid inhibitory  
 476 side-effects exerted on ET-capacity or even some uncoupling.

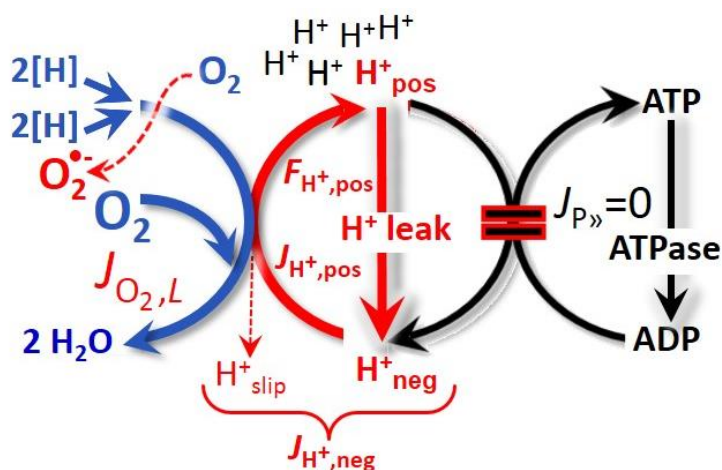


**Fig. 4. LEAK-state:** Phosphorylation is arrested,  $J_{P} = 0$ , and oxygen flux,  $J_{O_2,L}$ , is controlled mainly by the proton leak,  $J_{H^+,neg,L}$ , at maximum proton motive force,  $F_{H^+,pos}$ . See also Fig. 2 and 3.

477 Small differences of terms, *e.g.*, uncoupled *vs.* noncoupled, are easily overlooked,  
 478 although they relate to different mechanisms of uncoupling (**Fig. 3**). An attempt at rigorous  
 479 definition is required for clarification of concepts (**Table 2**).  
 480

481 **Table 2. Distinction of terms related to coupling and uncoupling (Fig. 3).**

Term	Respiration	P $\gg$ /O <sub>2</sub>	Note
Acoupled		0	Electron transfer in mitochondrial fragments without vectorial proton translocation
Uncoupled	<i>L</i>	0	Non-phosphorylating intrinsic LEAK-respiration, without added protonophore
 Uncoupled Decoupled Loosely coupled Dyscoupled		0	Component of LEAK-respiration, uncoupled <i>sui generis</i> , ion diffusion across the mtIM
		0	Component of LEAK-respiration, proton slip
		0	Component of LEAK-respiration, lower coupling due to superoxide anion radical formation and bypass of proton pumps
		0	Pathologically, toxicologically, environmentally increased uncoupling, mitochondrial dysfunction
Inducibly uncoupled	<i>E</i>	0	By UCP1 or cation ( <i>e.g.</i> Ca <sup>2+</sup> ) cycling
Noncoupled	<i>E</i>	0	Non-phosphorylating respiration stimulated to maximum flux at optimum exogenous uncoupler concentration ( <b>Fig. 6</b> )
Well-coupled	<i>P</i>	high	Phosphorylating respiration with an intrinsic LEAK component ( <b>Fig. 5</b> )
Fully coupled	<i>P – L</i>	max.	OXPPOS-capacity corrected for LEAK-respiration ( <b>Fig. 7</b> )

482  
 483 **Proton leak and uncoupled respiration:** Proton leak is a leak current of protons. The  
 484 intrinsic proton leak is the *uncoupled* process in which protons diffuse across the mtIM in the  
 485 dissipative direction of the downhill protonmotive force without coupling to phosphorylation  
 486 (**Fig. 4**). The proton leak flux depends non-linearly on the protonmotive force (Garlid *et al.*  
 487 1989; Divakaruni and Brand 2011), is a property of the mtIM, and may be enhanced due to  
 488 possible contaminations by free fatty acids. Inducible uncoupling mediated by uncoupling  
 489 protein 1 (UCP1) is physiologically controlled, *e.g.*, in brown adipose tissue. UCP1 is a member  
 490 of the mitochondrial carrier family which is involved in the translocation of protons across the  
 491 mtIM (Klingenberg 2017). As a consequence of this effective short-circuit, the protonmotive  
 492 force diminishes, resulting in stimulation of electron transfer to oxygen and heat dissipation  
 493 without phosphorylation of ADP.

494 **Cation cycling:** There can be other cation contributors to leak current including calcium  
 495 and probably magnesium. Calcium current is balanced by mitochondrial Na/Ca exchange,  
 496 which is balanced by Na/H exchange or K/H exchange. This is another effective uncoupling  
 497 mechanism different from proton leak and slip.

498 **Proton slip and decoupled respiration:** Proton slip is the *decoupled* process in which  
 499 protons are only partially translocated by a proton pump of the ET-pathways and slip back to  
 500 the original compartment. The proton leak is the dominant contributor to the overall leak current  
 501 in mammalian mitochondria incubated under physiological conditions at 37 °C, whereas proton

502 slip is increased at 25 °C (Dufour *et al.* 1996). Proton slip can also happen in association with  
 503 the ATP-synthase, in which case the proton slips downhill across the pump to the matrix without  
 504 contributing to ATP synthesis. In each case, proton slip is a property of the proton pump and  
 505 increases with the turnover rate of the pump.

506 **Electron leak and loosely coupled respiration:** Superoxide anion radical production by  
 507 the electron transfer system leads to a bypass of proton pumps and correspondingly lower  $P_{\gg}/O_2$   
 508 ratio, which depends on the actual site of electron leak and the scavenging of hydrogen peroxide  
 509 by cytochrome *c*, whereby electrons may re-enter the ET-system with proton translocation by  
 510 CIV.

511 **Loss of compartmental integrity and acoupled respiration:** Electron transfer and  $O_2$   
 512 consumption proceed without compartmental proton translocation in disrupted mitochondrial  
 513 fragments. Such fragments form during mitochondrial isolation, and may not fully fuse to re-  
 514 establish structurally intact mitochondria. Loss of mtIM integrity, therefore, is the cause of  
 515 acoupled respiration, which is a nonvectorial dissipative process without control by the  
 516 protonmotive force.

517 **Dyscoupled respiration:** Mitochondrial injuries may lead to *dyscoupling* as a  
 518 pathological or toxicological cause of *uncoupled* respiration. Dyscoupling may involve any  
 519 type of uncoupling mechanism, *e.g.*, opening the permeability transition pore. Dyscoupled  
 520 respiration is distinguished from the experimentally induced *noncoupled* respiration in the ET-  
 521 state (**Fig. 3**).

522

523 **OXPPOS-state (Fig. 5):**

524 The OXPPOS-state is defined as  
 525 the respiratory state with  
 526 kinetically-saturating  
 527 concentrations of  $O_2$ , respiratory  
 528 and phosphorylation substrates,  
 529 and absence of exogenous  
 530 uncoupler, which provides an  
 531 estimate of the maximal  
 532 respiratory capacity in the  
 533 OXPPOS-state for any given ET-  
 534 pathway state. Respiratory  
 535 capacities at kinetically-  
 536 saturating substrate  
 537 concentrations provide reference  
 538 values or upper limits of

539 performance, aiming at the generation of data sets for comparative purposes. Physiological  
 540 activities and effects of substrate kinetics can be evaluated relative to OXPPOS capacities.

541 As discussed previously, 0.2 mM ADP does not fully saturate flux in isolated  
 542 mitochondria (Gnaiger 2001; Puchowicz *et al.* 2004); greater ADP concentration is required,  
 543 particularly in permeabilized muscle fibres and cardiomyocytes, to overcome limitations by  
 544 intracellular diffusion and by the reduced conductance of the mitochondrial outer membrane,  
 545 mtOM (Jepihhina *et al.* 2011, Illaste *et al.* 2012, Simson *et al.* 2016), either through interaction  
 546 with tubulin (Rostovtseva *et al.* 2008) or other intracellular structures (Birkedal *et al.* 2014). In  
 547 permeabilized muscle fibre bundles of high respiratory capacity, the apparent  $K_m$  for ADP  
 548 increases up to 0.5 mM (Saks *et al.* 1998), indicating that >90% saturation is reached only at  
 549 >5 mM ADP. Similar ADP concentrations are also required for accurate determination of  
 550 OXPPOS-capacity in human clinical cancer samples and permeabilized cells (Klepinin *et al.*  
 551 2016; Koit *et al.* 2017). Whereas 2.5 to 5 mM ADP is sufficient to obtain the actual OXPPOS-

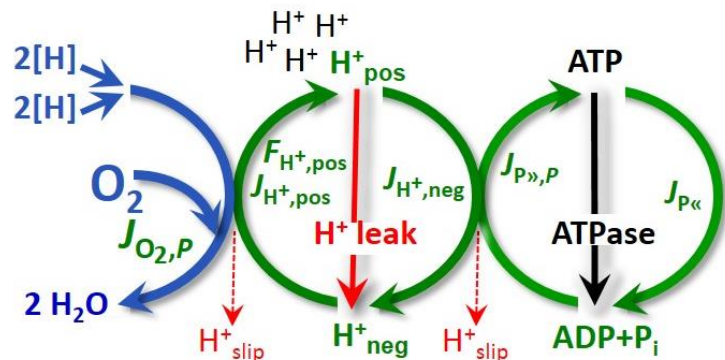


**Fig. 5. OXPPOS-state:** Phosphorylation,  $J_{P_{\gg}}$ , is stimulated by kinetically-saturating [ADP] and inorganic phosphate,  $[P_i]$ , and is supported by a high protonmotive force,  $F_{H^+,pos}$ .  $O_2$  flux,  $J_{O_2,P}$ , is well-coupled at a  $P_{\gg}/O_2$  ratio of  $J_{P_{\gg},P}/J_{O_2,P}$ . See also Fig. 2.

552 capacity in many types of permeabilized tissue and cell preparations, experimental validation  
 553 is required in each specific case.

554

555 **Electron transfer-state**  
 556 (Fig. 6): The ET-state is defined  
 557 as the *noncoupled* state with  
 558 kinetically-saturating  
 559 concentrations of O<sub>2</sub>, respiratory  
 560 substrate and optimum  
 561 *exogenous* uncoupler  
 562 concentration for maximum O<sub>2</sub>  
 563 flux, as an estimate of oxidative  
 564 ET-capacity. Inhibition of  
 565 respiration is observed at higher  
 566 than optimum uncoupler  
 567 concentrations. As a  
 568 consequence of the nearly  
 569 collapsed protonmotive force, the  
 570 driving force is insufficient for  
 571 phosphorylation, and  $J_{P_{\gg}} = 0$ .

572

573 Besides the three fundamental coupling states of mitochondrial preparations, the  
 574 following respiratory state also is relevant to assess respiratory function:

575

576 **ROX state and *Rox***: Residual oxygen consumption, *Rox*, is defined as O<sub>2</sub> consumption  
 577 due to oxidative side reactions remaining after inhibition of ET with rotenone, malonic acid and  
 578 antimycin A. Cyanide and azide not only inhibit CIV but several peroxidases which should be  
 579 involved in *Rox*. ROX is not a coupling state. *Rox* represents a baseline that is used to correct  
 580 mitochondrial respiration in defined coupling states. *Rox* is not necessarily equivalent to non-  
 581 mitochondrial respiration, considering oxygen-consuming reactions in mitochondria not related  
 582 to ET, such as oxygen consumption in reactions catalyzed by monoamine oxidases (type A and  
 583 B), monooxygenases (cytochrome P450 monooxygenases), dioxygenase (sulfur dioxygenase  
 584 and trimethyllysine dioxygenase), several hydroxylases, and more. Mitochondrial preparations,  
 585 especially those obtained from liver, may be contaminated by peroxisomes. This fact makes the  
 586 exact determination of mitochondrial oxygen consumption and mitochondria-associated  
 587 generation of reactive oxygen species complicated (Schönfeld *et al.* 2009). The dependence of  
 588 ROX-linked oxygen consumption needs to be studied in detail with respect to non-ET enzyme  
 589 activities, availability of specific substrates, oxygen concentration, and electron leakage leading  
 590 to the formation of reactive oxygen species.

591

## 592 2.2. Coupling states and respiratory rates

593

594 It is important to distinguish metabolic *pathways* from metabolic *states* and the  
 595 corresponding metabolic *rates*; for example: ET-pathways (Fig. 7), ET-state (Fig. 6), and ET-  
 596 capacity, *E*, respectively (Table 1). The protonmotive force is *high* in the OXPHOS-state when  
 597 it drives phosphorylation, *maximum* in the LEAK-state of coupled mitochondria, driven by  
 598 LEAK-respiration at a minimum back flux of cations to the matrix side, and *very low* in the ET-  
 599 state when uncouplers short-circuit the proton cycle (Table 1).

600 The three coupling states, ET, LEAK and OXPHOS, are shown schematically with the  
 601 corresponding respiratory rates, abbreviated as *E*, *L* and *P*, respectively (Fig. 7). *E* may exceed  
 602 or be equal to *P*, but *E* cannot theoretically be lower than *P*.  $E < P$  must be discounted as an

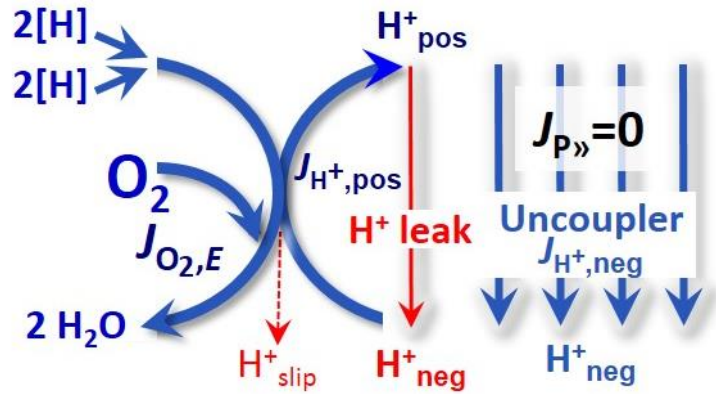


Fig. 6. ET-state: Noncoupled respiration,  $J_{O_{2,E}}$ , is maximum at optimum exogenous uncoupler concentration and phosphorylation is zero,  $J_{P_{\gg}} = 0$ . See also Fig. 2.

603 artefact, which may be caused experimentally by: (1) loss of oxidative capacity during the time  
 604 course of the respirometric assay, since  $E$  is measured subsequently to  $P$ ; (2) using insufficient  
 605 uncoupler concentrations; (3) using high uncoupler concentrations which inhibit ET (Gnaiger  
 606 2008); (4) high oligomycin concentrations applied for measurement of  $L$  before titrations of  
 607 uncoupler, when oligomycin exerts an inhibitory effect on  $E$ . On the other hand, the excess ET-  
 608 capacity is overestimated if non-saturating [ADP] or  $[P_i]$  are used. See State 3 in the next  
 609 section.

610

611 **Fig. 7. Four-compartment model of oxidative phosphorylation.**

612 Respiratory states (ET, OXPHOS, LEAK) and corresponding rates ( $E$ ,  $P$ ,  $L$ )  
 613 are connected by the protonmotive force,  $F_{H^+}$ . Electron  
 614 transfer-capacity,  $E$ , is partitioned  
 615 into (1) dissipative LEAK-  
 616 respiration,  $L$ , when the Gibbs  
 617 energy change of catabolic  $O_2$

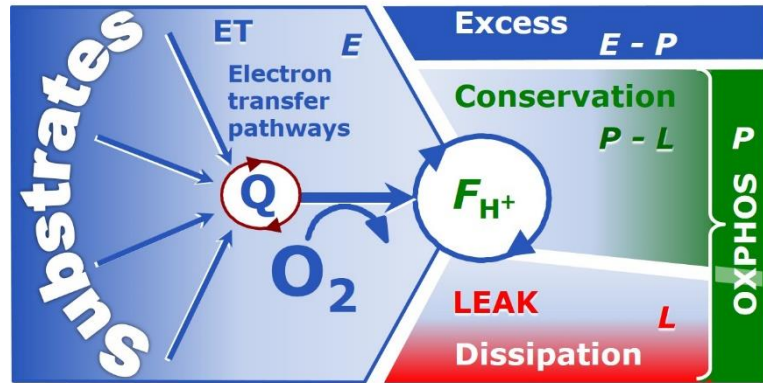
618 consumption is irreversibly lost, (2) net OXPHOS-capacity,  $P-L$ , with partial conservation of  
 619 the capacity to perform work, and (3) the excess capacity,  $E-P$ . Modified from Gnaiger (2014).

622

623  
 624  
 625  $E > P$  is observed in many types of mitochondria, varying between species, tissues and  
 626 cell types.  $E-P$  is the excess ET-capacity pushing the phosphorylation-flux (Fig. 1B) to the limit  
 627 of its *capacity of utilizing* the protonmotive force. Within any type of mitochondria, the  
 628 magnitude of  $E-P$  depends on: (1) the pathway control state with single or multiple electron  
 629 input into the Q-junction and involvement of three or fewer coupling sites determining the  
 630  $H^+_{pos}/O_2$  coupling stoichiometry (Fig. 1A); and (2) the biochemical coupling efficiency  
 631 expressed as  $(E-L)/E$ , since an increase of  $L$  causes  $P$  to increase towards the limit of  $E$ . The  
 632 excess  $E-P$  capacity,  $E-P$ , therefore, provides a sensitive diagnostic indicator of specific injuries  
 633 of the phosphorylation-pathway, under conditions when  $E$  remains constant but  $P$  declines  
 634 relative to controls (Fig. 7). Substrate cocktails supporting simultaneous convergent electron  
 635 transfer to the Q-junction for reconstitution of tricarboxylic acid cycle (TCA cycle) function  
 636 establish pathway control states with high ET-capacity, and consequently increase the  
 637 sensitivity of the  $E-P$  assay.

638 When subtracting  $L$  from  $P$ , the dissipative LEAK component in the OXPHOS-state may  
 639 be overestimated. This can be avoided by measuring LEAK-respiration in a state when the  
 640 protonmotive force is adjusted to its slightly lower value in the OXPHOS-state, e.g., by titration  
 641 of an ET inhibitor (Divakaruni and Brand 2011). Any turnover-dependent components of  
 642 proton leak and slip, however, are underestimated under these conditions (Garlid *et al.* 1993).  
 643 In general, it is inappropriate to use the term *ATP production* or *ATP turnover* for the difference  
 644 of oxygen consumption measured in states  $P$  and  $L$ . The difference  $P-L$  is the upper limit of the  
 645 part of OXPHOS-capacity that is freely available for ATP production (corrected for LEAK-  
 646 respiration) and is fully coupled to phosphorylation with a maximum mechanistic stoichiometry  
 647 (Fig. 7).

648



## 649 2.3. Classical terminology for isolated mitochondria

650 'When a code is familiar enough, it ceases appearing like a code; one forgets that  
651 there is a decoding mechanism. The message is identical with its meaning'  
652 (Hofstadter 1979).

653

654 Chance and Williams (1955; 1956) introduced five classical states of mitochondrial respiration  
655 and cytochrome redox states. **Table 3** shows a protocol with isolated mitochondria in a closed  
656 respirometric chamber, defining a sequence of respiratory states.

657

658

**Table 3. Metabolic states of mitochondria (Chance and Williams, 1956; Table V).**

State	[O <sub>2</sub> ]	ADP level	Substrate Level	Respiration rate	Rate-limiting substance
1	>0	low	low	slow	ADP
2	>0	high	~0	slow	substrate
3	>0	high	high	fast	respiratory chain
4	>0	low	high	slow	ADP
5	0	high	high	0	oxygen

661

662 **State 1** is obtained after addition of isolated mitochondria to air-saturated  
663 isoosmotic/isotonic respiration medium containing inorganic phosphate, but no fuel substrates  
664 and no adenylates, *i.e.*, AMP, ADP, ATP.

665 **State 2** is induced by addition of a high concentration of ADP (typically 100 to 300  $\mu$ M),  
666 which stimulates respiration transiently on the basis of endogenous fuel substrates and  
667 phosphorylates only a small portion of the added ADP. State 2 is then obtained at a low  
668 respiratory activity limited by exhausted endogenous fuel substrate availability (**Table 3**). If  
669 addition of specific inhibitors of respiratory complexes, such as rotenone, does not cause a  
670 further decline of oxygen consumption, State 2 is equivalent to residual oxygen consumption  
671 (See below.). If inhibition is observed, undefined endogenous fuel substrates are a confounding  
672 factor of pathway control, contributing to the effect of subsequently externally added substrates  
673 and inhibitors. In contrast to the original protocol, an alternative sequence of titration steps is  
674 frequently applied, in which the alternative 'State 2' has an entirely different meaning, when  
675 this second state is induced by addition of fuel substrate without ADP (LEAK-state; in contrast  
676 to State 2 defined in **Table 1** as a ROX state), followed by addition of ADP.

677 **State 3** is the state stimulated by addition of fuel substrates while the ADP concentration  
678 is still high (**Table 3**) and supports coupled energy transformation through oxidative  
679 phosphorylation. 'High ADP' is a concentration of ADP specifically selected to allow the  
680 measurement of State 3 to State 4 transitions of isolated mitochondria in a closed respirometric  
681 chamber. Repeated ADP titration re-establishes State 3 at 'high ADP'. Starting at oxygen  
682 concentrations near air-saturation (ca. 200  $\mu$ M O<sub>2</sub> at sea level and 37 °C), the total ADP  
683 concentration added must be low enough (typically 100 to 300  $\mu$ M) to allow phosphorylation  
684 to ATP at a coupled rate of oxygen consumption that does not lead to oxygen depletion during  
685 the transition to State 4. In contrast, kinetically-saturating ADP concentrations usually are an  
686 order of magnitude higher than 'high ADP', *e.g.* 2.5 mM in isolated mitochondria. The  
687 abbreviation State 3u is occasionally used in bioenergetics, to indicate the state of respiration  
688 after titration of an uncoupler, without sufficient emphasis on the fundamental difference  
689 between OXPHOS-capacity (*well-coupled* with an *endogenous* uncoupled component) and ET-  
690 capacity (*noncoupled*).



691 **State 4** is a LEAK-state that is obtained only if the mitochondrial preparation is intact  
 692 and well-coupled. Depletion of ADP by phosphorylation to ATP leads to a decline in the rate  
 693 of oxygen consumption in the transition from State 3 to State 4. Under these conditions, a  
 694 maximum protonmotive force and high ATP/ADP ratio are maintained, and the  $P_{\gg}/O_2$  ratio can  
 695 be calculated. State 4 respiration,  $L_T$  (**Table 1**), reflects intrinsic proton leak and intrinsic ATP  
 696 hydrolysis activity. Oxygen consumption in State 4 is an overestimation of LEAK-respiration  
 697 if the contaminating ATP hydrolysis activity recycles some ATP to ADP,  $J_{P\ll}$ , which stimulates  
 698 respiration coupled to phosphorylation,  $J_{P\gg} > 0$ . This can be tested by inhibition of the  
 699 phosphorylation-pathway using oligomycin, ensuring that  $J_{P\gg} = 0$  (State 4o). Alternatively,  
 700 sequential ADP titrations re-establish State 3, followed by State 3 to State 4 transitions while  
 701 sufficient oxygen is available. However, anoxia may be reached before exhaustion of ADP  
 702 (State 5).

703 **State 5** is the state after exhaustion of oxygen in a closed respirometric chamber.  
 704 Diffusion of oxygen from the surroundings into the aqueous solution may be a confounding  
 705 factor preventing complete anoxia (Gnaiger 2001). Chance and Williams (1955) provide an  
 706 alternative definition of State 5, which gives it the meaning of ROX: ‘State 5 may be obtained  
 707 by antimycin A treatment or by anaerobiosis’.

708 In **Table 3**, only States 3 and 4 (and ‘State 2’ in the alternative protocol without ADP;  
 709 not included in the table) are coupling control states, with the restriction that  $O_2$  flux in State 3  
 710 may be limited kinetically by non-saturating ADP concentrations (**Table 1**).

711

### 712 3. The protonmotive force and proton flux

713

#### 714 3.1. Electric and chemical partial forces versus electrical and chemical units

715

716 The protonmotive force across the mtIM (Mitchell 1961; Mitchell and Moyle 1967) was  
 717 introduced most beautifully in the *Grey Book 1966* (Mitchell 2011),

$$718 \Delta p = \Delta \Psi + \Delta \mu_{H^+}/F \quad (\text{Eq. 1})$$

719 The protonmotive force,  $\Delta p$ , consists of two partial forces: (1) The electric part,  $\Delta \Psi$ , is the  
 720 difference of charge (electric potential difference), is not specific for  $H^+$ , and can, therefore, be  
 721 measured by the distribution of other permeable cations between the positive and negative  
 722 compartment (**Fig. 2**). (2) The chemical part contains the chemical potential difference in  $H^+$ ,  
 723  $\Delta \mu_{H^+}$ , which is proportional to the pH difference,  $\Delta pH$  (**Table 4**).

724 **Faraday constant**,  $F = e \cdot N_A$  [C/mol] (**Table 4**, note 1) enables the conversion between  
 725 protonmotive force,  $F_{H^+/e} \equiv \Delta p$  [J/C], expressed per *motive charge*,  $e$  [C], and protonmotive  
 726 force,  $F_{H^+/n} \equiv \Delta \tilde{\mu}_{H^+} = \Delta p \cdot F$  [J/mol], expressed per *motive amount of protons*,  $n$  [mol]. Proton  
 727 charge,  $e$ , and amount of substance,  $n$ , are motive entities expressed in units C and mol,  
 728 respectively. Taken together,  $F$  is the conversion factor for expressing protonmotive force and  
 729 flux in motive units of  $e$  or  $n$  (Eq. 2; **Table 4**, Notes 1 and 2),

$$730 F_{H^+/n} = F_{H^+/e} \cdot (e \cdot N_A) \quad (\text{Eq. 2.1})$$

$$731 J_{H^+/n} = J_{H^+/e} / (e \cdot N_A) \quad (\text{Eq. 2.2})$$

732 In each format, the protonmotive force is expressed as the sum of two partial isomorphic  
 733 forces. The complex symbols in Eq. 1 can be explained and visualized more explicitly by  
 734 *partial isomorphic forces* as the components of the protonmotive force:

735 **Electric part of the protonmotive force:** (1) Isomorph  $e$ :  $F_{el/e} \equiv \Delta \Psi$  is the electric part  
 736 of the protonmotive force expressed in electrical units joule per coulomb, *i.e.* volt [V = J/C].  
 737  $F_{el/e}$  is defined as partial Gibbs energy change per *motive elementary charge*,  $e$  [C], not specific  
 738 for proton charge (**Table 4**, Note 2e). (2) Isomorph  $n$ :  $F_{el/n} \equiv \Delta \Psi \cdot F$  is the electric force expressed  
 739 in chemical units joule per mole [J/mol], defined as partial Gibbs energy change per *motive*  
 740 *amount of charge*,  $n$  [mol], not specific for proton charge (**Table 4**, Note 2n).

741 **Chemical part of the protonmotive force:** (1) Isomorph  $n$ :  $F_{H^+,d/n} \equiv \Delta\mu_{H^+}$  is the chemical  
 742 part (diffusion, displacement of  $H^+$ ) of the protonmotive force expressed in units joule per mole  
 743 [J/mol].  $F_{H^+,d/n}$  is defined as partial Gibbs energy change per *motive amount of protons*,  $n$  [mol]  
 744 (**Table 4**, Note 2n). (2) Isomorph  $e$ :  $F_{H^+,d/e} \equiv \Delta\mu_{H^+}/F$  is the chemical force expressed in units  
 745 joule per coulomb [J/C = V], defined as partial Gibbs energy change per *motive amount of*  
 746 *protons expressed in units of electric charge*,  $e$  [C], but specific for proton charge (**Table 4**,  
 747 Note 2e).

748

749 **Table 4. Protonmotive force and flux matrix.** Columns: The protonmotive force is  
 750 the sum of two *partial isomorphic forces*,  $F_{el} + F_{H^+,d}$ . Rows: Electrical and chemical  
 751 formats (motive units, MU: C and mol, for  $e$  and  $n$ , respectively). The Faraday constant,  
 752  $F$ , converts protonmotive force and flux from format  $e$  to  $n$ . In contrast to force (state),  
 753 the conjugated flux (rate) cannot be partitioned.

754

State	Force	electric	+	chem.	Unit	Notes	
Protonmotive force, $e$	$\Delta p$	=	$\Delta\Psi$	+ $\Delta\mu_{H^+}/F$	$J\cdot C^{-1}$	1e	
Chemiosmotic potential, $n$	$\Delta\tilde{\mu}_{H^+}$	=	$\Delta\Psi\cdot F$	+ $\Delta\mu_{H^+}$	$J\cdot mol^{-1}$	1n	
State	Isomorphic force	$F_{H^+}$	el	+	$H^+_d$	$J\cdot MU^{-1}$	
Electric charge, $e$	$F_{H^+/e}$	=	$F_{el/e}$	+	$F_{H^+,d/e}$	$J\cdot C^{-1}$	2e
Amount of substance, $n$	$F_{H^+/n}$	=	$F_{el/n}$	+	$F_{H^+,d/n}$	$J\cdot mol^{-1}$	2n
Rate	Isomorphic flux	$J_{H^+}$	$e$	or	$n$	$MU\cdot s^{-1}\cdot m^{-3}$	
Electric charge, $e$	$J_{H^+/e}$		$J_{H^+/e}$			$C\cdot s^{-1}\cdot m^{-3}$	3e
Amount of substance, $n$	$J_{H^+/n}$				$J_{H^+/n}$	$mol\cdot s^{-1}\cdot m^{-3}$	3n

755

756 1: The Faraday constant,  $F$ , is the product of elementary charge ( $e = 1.602\ 176\ 634\cdot 10^{-19}$  C) and the  
 757 Avogadro (Loschmidt) constant ( $N_A = 6.022\ 140\ 76\cdot 10^{23}$  mol $^{-1}$ ),  $F = e\cdot N_A = 96,485.33$  C $\cdot$ mol $^{-1}$  (Gibney

758 2017).  $F$  is the conversion factor between electrical and chemical units.  $\Delta\tilde{\mu}_{H^+}$  is the chemiosmotic  
 759 potential difference. 1e and 1n are the classical representations of 2e and 2n.

760 2:  $F_{H^+}$  is the protonmotive force expressed in formats  $e$  [C] or  $n$  [mol].  $F_{el/e} \equiv \Delta\Psi$  is the partial  
 761 protonmotive force (el) acting generally on charged motive molecules (*i.e.* ions that are permeable  
 762 across the mtIM). In contrast,  $F_{H^+,d/n} \equiv \Delta\mu_{H^+}$  is the partial protonmotive force specific for proton  
 763 diffusion,  $H^+_d$ , irrespective of charge. The sign of the force is negative for exergonic transformations  
 764 in which exergy is lost or dissipated,  $F_{H^+,neg}$ , and positive for endergonic transformations which  
 765 conserve exergy in a coupled exergonic process,  $F_{H^+,pos} = -F_{H^+,neg}$  (**Box 3**).

766 3: The sign of the flux,  $J_{H^+}$ , depends on the definition of the compartmental direction of the translocation.  
 767 Flux in the outward direction into the positively (pos) charged compartment,  $J_{H^+,pos}$ , is positive when  
 768  $H^+_{pos}$  is added to the pos-compartment ( $v_{H^+,pos} = 1$ ), and  $H^+_{neg}$  is removed stoichiometrically ( $v_{H^+,neg}$   
 769 = -1). Conversely,  $J_{H^+,neg}$  is positive when  $H^+_{neg}$  is added to the negatively charged compartment  
 770 ( $v_{H^+,neg} = 1$ ) and  $H^+_{pos}$  is removed ( $v_{H^+,pos} = -1$ ; **Fig. 2**). By definition, the product of flux and force is  
 771 volume-specific power [ $J\cdot s^{-1}\cdot m^{-3} = W\cdot m^{-3}$ ]:  $P_{V,H^+} = J_{H^+,pos/e}\cdot F_{H^+,pos/e} = J_{H^+,pos/n}\cdot F_{H^+,pos/n}$ .

772

773 Protonmotive means that there is a potential for the movement of protons, and force is a  
 774 measure of the potential for motion. Motion is relative and not absolute (Principle of Galilean  
 775 Relativity); likewise there is no absolute potential, but isomorphic forces are potential  
 776 differences (**Table 5**, Notes 5 and 6),

$$777 F_{el/n} = \Delta\psi\cdot zF = RT\cdot\Delta\ln c_{Bz} \quad (\text{Eq. 3.1})$$

$$778 F_{H^+,d/n} = \Delta\mu_{H^+} = RT\cdot\Delta\ln c_{H^+} \quad (\text{Eq. 3.2})$$

779 The isomorphism of the electric and chemical partial forces is most clearly illustrated when  
 780 expressing all terms (Eq. 3) as dimensionless quantities (Eq. 4). For diffusion of protons into  
 781 the matrix space (**Fig. 2**),

$$782 F_{el,neg/n}\cdot RT^{-1} = \ln(c_{Bz,pos}/c_{Bz,neg}) \quad (\text{Eq. 4.1})$$

$$783 F_{H^+,neg,d/n}\cdot RT^{-1} = \ln(c_{H^+,pos}/c_{H^+,neg}) \quad (\text{Eq. 4.2})$$

784

**Table 5. Power, exergy, force, flux, and advancement.**

Expression	Symbol	Definition	Unit	Notes
Power, volume-specific	$P_{V, \text{tr}}$	$P_{V, \text{tr}} = J_{\text{tr}} \cdot F_{\text{tr}} = d_{\text{tr}} G \cdot dt^{-1}$	$\text{W} \cdot \text{m}^{-3} = \text{J} \cdot \text{s}^{-1} \cdot \text{m}^{-3}$	1
Force, isomorphic	$F_{\text{tr}}$	$F_{\text{tr}} = \partial G / \partial \xi_{\text{tr}}$	$\text{J} \cdot \text{MU}^{-1}$	2
Flux, isomorphic	$J_{\text{tr}}$	$J_{\text{tr}} = d_{\text{tr}} \xi_{\text{tr}} \cdot dt^{-1} \cdot V^{-1}$	$\text{MU} \cdot \text{s}^{-1} \cdot \text{m}^{-3}$	3
Advancement, $n$	$d_{\text{tr}} \xi_{\text{H}^+/n}$	$d_{\text{tr}} \xi_{\text{H}^+/n} = d_{\text{tr}} n_{\text{H}^+} \cdot \nu_{\text{H}^+}^{-1}$	$\text{MU} = \text{mol}$	$4n$
Advancement, $e$	$d_{\text{tr}} \xi_{\text{H}^+/e}$	$d_{\text{tr}} \xi_{\text{H}^+/e} = d_{\text{tr}} e_{\text{H}^+} \cdot \nu_{\text{H}^+}^{-1}$	$\text{MU} = \text{C}$	$4e$
Electric partial force, $e$	$F_{\text{el}/e}$	$F_{\text{el}/e} \equiv \Delta \Psi = RT / (zF) \cdot \Delta \ln a_{\text{B}z}$	$\text{V} = \text{J} \cdot \text{C}^{-1}$	$5e$
Electric partial force, $n$	$F_{\text{el}/n}$	$F_{\text{el}/n} \equiv \Delta \Psi \cdot zF = RT \cdot \Delta \ln a_{\text{B}z}$	$\text{kJ} \cdot \text{mol}^{-1}$	$5n$
	at $z = 1$	$= 96.5 \cdot \Delta \Psi$	$\text{kJ} \cdot \text{mol}^{-1}$	
Chemical partial force, $e$	$F_{\text{H}^+, \text{d}/e}$	$F_{\text{H}^+, \text{d}/e} \equiv \Delta \mu_{\text{H}^+} / F = -RT / F \cdot \ln(10) \cdot \Delta \text{pH}$	$\text{J} \cdot \text{C}^{-1}$	$6e$
	at $37^\circ \text{C}$	$= -0.061 \cdot \Delta \text{pH}$	$\text{J} \cdot \text{C}^{-1}$	
Chemical partial force, $n$	$F_{\text{H}^+, \text{d}/n}$	$F_{\text{H}^+, \text{d}/n} \equiv \Delta \mu_{\text{H}^+} = -RT \cdot \ln(10) \cdot \Delta \text{pH}$	$\text{J} \cdot \text{mol}^{-1}$	$6n$
	at $37^\circ \text{C}$	$= -5.9 \cdot \Delta \text{pH}$	$\text{kJ} \cdot \text{mol}^{-1}$	

787

788 1 to 4: A motive entity, expressed in a motive unit [MU] is a characteristic for any type of transformation,  
789 tr.  $\text{MU} = \text{mol}$  or  $\text{C}$  in the chemical or electrical format of proton translocation.

790 2: Isomorphic forces,  $F_{\text{tr}}$ , are related to the generalized forces,  $X_{\text{tr}}$ , of irreversible thermodynamics  
791 as  $F_{\text{tr}} = -X_{\text{tr}} \cdot T$ , and the force of chemical reactions is the negative affinity,  $F_{\text{r}} = -A$  (Prigogine 1967).  
792  $\partial G$  [J] is the partial Gibbs energy change in the advancement of transformation tr.

793 3: For  $\text{MU} = \text{C}$ , flow is electric current,  $I_{\text{el}}$  [ $\text{A} = \text{C} \cdot \text{s}^{-1}$ ], vector flux is electric current density per area,  
794  $\mathbf{J}_{\text{el}}$ , and compartmental flux is electric current density per volume,  $i_{\text{el}}$  [ $\text{A} \cdot \text{m}^{-3}$ ], all expressed in  
795 electrical format.

796  $4n$ : For a chemical reaction, the advancement of reaction  $r$  is  $d_r \xi_{\text{B}} = d_r n_{\text{B}} \cdot \nu_{\text{B}}^{-1}$  [mol]. The stoichiometric  
797 number is  $\nu_{\text{B}} = -1$  or  $\nu_{\text{B}} = 1$ , depending on B being a product or substrate, respectively, in reaction  
798  $r$  involving one mole of B. The conjugated *intensive* molar quantity,  $F_{\text{B}, r} = \partial G / \partial \xi_{\text{B}}$  [ $\text{J} \cdot \text{mol}^{-1}$ ], is the  
799 chemical force of reaction or *reaction-motive* force per stoichiometric amount of B. In reaction  
800 kinetics,  $d_r n_{\text{B}}$  is expressed as a volume-specific quantity, which is the partial contribution to the  
801 total concentration change of B,  $d_r c_{\text{B}} = d_r n_{\text{B}} / V$  and  $dc_{\text{B}} = dn_{\text{B}} / V$ , respectively. In open systems with  
802 constant volume  $V$ ,  $dc_{\text{B}} = d_r c_{\text{B}} + d_e c_{\text{B}}$ , where  $r$  indicates the *internal* reaction and  $e$  indicates the  
803 *external* flux of B into the unit volume of the system. At steady state the concentration does not  
804 change,  $dc_{\text{B}} = 0$ , when  $d_r c_{\text{B}}$  is compensated for by the external flux of B,  $d_r c_{\text{B}} = -d_e c_{\text{B}}$  (Gnaiger  
805 1993b). Alternatively,  $dc_{\text{B}} = 0$  when B is held constant by different coupled reactions in which B  
806 acts as a substrate or a product.

807  $4e$ : Scalar potential difference across the mitochondrial membrane. In a scalar electric transformation  
808 (flux of charge, *i.e.* volume-specific current, from the matrix space to the intermembrane and  
809 extramitochondrial space), the motive force is the difference of charge (**Box 2**). The endergonic  
810 direction of translocation is defined in **Fig. 2** as  $\text{H}^+_{\text{neg}} \rightarrow \text{H}^+_{\text{pos}}$ .

811  $5e$ :  $F = 96.5$  ( $\text{kJ} \cdot \text{mol}^{-1}$ ) /  $V$ .  $z_{\text{B}}$  is the charge number of ion B.  $a_{\text{B}}$  is the (relative) activity of ion B, which  
812 in dilute solutions ( $c < 0.1$   $\text{mol} \cdot \text{dm}^{-3}$ ) is approximately equal to  $c_{\text{B}} / c^\circ$ , where  $c^\circ$  is the standard  
813 concentration of  $1$   $\text{mol} \cdot \text{dm}^{-3}$ .  $\Delta \ln a_{\text{B}} = \ln a_2 - \ln a_1 = \ln(a_2 / a_1)$ , when ion B diffuses or is translocated  
814 from compartment 1 to 2 (Eq. 4). Compartments 1 and 2 have to be defined in each case (**Fig.**  
815 **2**). Note that ion selective electrodes (pH or  $\text{TPP}^+$  electrodes) respond to  $\ln a_{\text{B}}$ .  $\Delta \ln a_{\text{H}^+} = -$   
816  $\ln(10) \cdot \Delta \text{pH}$ .

- 817 6:  $R = 8.31451 \text{ J}\cdot\text{mol}^{-1}\cdot\text{K}^{-1}$  is the gas constant.  $RT = 2.479$  and  $2.579 \text{ kJ}\cdot\text{mol}^{-1}$  at  $298.15$  and  $310.15$   
 818 K ( $25$  and  $37 \text{ }^\circ\text{C}$ ), respectively. See Eq. 3 and 4.  
 819 6e:  $RT/F\Delta\ln a_{\text{H}^+}$  yields force in the electrical format [ $\text{J}\cdot\text{C}^{-1} = \text{V}$ ].  $RT/F = 2.479$  and  $2.579 \text{ mV}$  at  $298.15$   
 820 and  $310.15 \text{ K}$ , respectively, and  $\ln(10)\cdot RT/F = 59.16$  and  $61.54 \text{ mV}$ , respectively.  
 821 6n:  $RT\Delta\ln a_{\text{H}^+}$  yields force in the chemical format [ $\text{J}\cdot\text{mol}^{-1}$ ].  $\ln(10)\cdot RT = 5.708$  and  $5.938 \text{ kJ}\cdot\text{mol}^{-1}$  at  
 822  $298.15$  and  $310.15 \text{ K}$ , respectively.  
 823

824 An electric partial force of  $0.2 \text{ V}$ , expressed in the format of electric charge,  $F_{\text{el, pos/e}}$  (**Table**  
 825 **5**, Note 5e), can be expressed equivalently as  $19 \text{ kJ}\cdot\text{mol}^{-1} \text{ H}^+_{\text{pos}}$ , in the format of amount,  $F_{\text{el, pos/n}}$   
 826 (Note 5n). For a  $\Delta\text{pH}$  of 1 unit, the chemical partial force in the format of amount,  $F_{\text{H}^+, \text{pos, d/n}}$ ,  
 827 changes by  $5.9 \text{ kJ}\cdot\text{mol}^{-1}$  (**Table 5**, Note 6n), and chemical force in the format of charge,  
 828  $F_{\text{H}^+, \text{pos, d/e}}$ , changes by  $0.06 \text{ V}$  (Note 6e). Considering a driving force of  $-470 \text{ kJ}\cdot\text{mol}^{-1} \text{ O}_2$  for  
 829 oxidation, the thermodynamic limit of the  $\text{H}^+_{\text{pos}}/\text{O}_2$  ratio is reached at a value of  $470/19 = 24$ ,  
 830 compared to a mechanistic stoichiometry of 20 (**Fig. 1**).  
 831

### 832 3.2. Definitions

834 **Control and regulation:** The terms metabolic *control* and *regulation* are frequently used  
 835 synonymously, but are distinguished in metabolic control analysis: ‘We could understand the  
 836 regulation as the mechanism that occurs when a system maintains some variable constant over  
 837 time, in spite of fluctuations in external conditions (homeostasis of the internal state). On the  
 838 other hand, metabolic control is the power to change the state of the metabolism in response to  
 839 an external signal’ (Fell 1997). Respiratory control may be induced by experimental control  
 840 signals that *exert* an influence on: (1) ATP demand and ADP phosphorylation-rate; (2) fuel  
 841 substrate composition, pathway competition; (3) available amounts of substrates and oxygen,  
 842 *e.g.*, starvation and hypoxia; (3) the protonmotive force, redox states, flux-force relationships,  
 843 coupling and efficiency; (4)  $\text{Ca}^{2+}$  and other ions including  $\text{H}^+$ ; (5) inhibitors, *e.g.*, nitric oxide  
 844 or intermediary metabolites, such as oxaloacetate; (6) signalling pathways and regulatory  
 845 proteins, *e.g.* insulin resistance, transcription factor HIF-1 or inhibitory factor 1. *Mechanisms*  
 846 of respiratory control and regulation include adjustments of: (1) enzyme activities by allosteric  
 847 mechanisms and phosphorylation; (2) enzyme content, concentrations of cofactors and  
 848 conserved moieties (such as adenylates, nicotinamide adenine dinucleotide [ $\text{NAD}^+/\text{NADH}$ ],  
 849 coenzyme Q, cytochrome *c*); (3) metabolic channeling by supercomplexes; and (4)  
 850 mitochondrial density (enzyme concentrations and membrane area) and morphology (cristae  
 851 folding, fission and fusion). (5) Mitochondria are targeted directly by hormones, thereby  
 852 affecting their energy metabolism (Lee *et al.* 2013; Gerö and Szabo 2016; Price and Dai 2016;  
 853 Moreno *et al.* 2017). Evolutionary or acquired differences in the genetic and epigenetic basis  
 854 of mitochondrial function (or dysfunction) between subjects and gene therapy; age; gender,  
 855 biological sex, and hormone concentrations; life style including exercise and nutrition; and  
 856 environmental issues including thermal, atmospheric, toxicological and pharmacological  
 857 factors, exert an influence on all control mechanisms listed above. For reviews, see Brown  
 858 1992; Gnaiger 1993a, 2009; 2014; Paradies *et al.* 2014; Morrow *et al.* 2017.

859 **Respiratory control and response:** Lack of control by a metabolic pathway, *e.g.*  
 860 phosphorylation-pathway, does mean that there will be no response to a variable activating it,  
 861 *e.g.* [ADP]. However, the reverse is not true as the absence of a response to [ADP] does not  
 862 exclude the phosphorylation-pathway from having some degree of control. The degree of  
 863 control of a component of the OXPHOS-pathway on an output variable, such as oxygen flux,  
 864 will in general be different from the degree of control on other outputs, such as phosphorylation-  
 865 flux or proton leak flux (**Box 2**). As such, it is necessary to be specific as to which input and  
 866 output are under consideration (Fell 1997). Therefore, the term respiratory control is elaborated  
 867 in more detail in the following section.

868 **Respiratory coupling control:** Respiratory control refers to the ability of mitochondria  
 869 to adjust oxygen consumption in response to external control signals by engaging various  
 870 mechanisms of control and regulation. Respiratory control is monitored in a mitochondrial  
 871 preparation under conditions defined as respiratory states. When phosphorylation of ADP to  
 872 ATP is stimulated or depressed, an increase or decrease is observed in electron flux linked to  
 873 oxygen consumption in respiratory coupling states of intact mitochondria ('controlled states' in  
 874 the classical terminology of bioenergetics). Alternatively, coupling of electron transfer with  
 875 phosphorylation is disengaged by disruption of the integrity of the mtIM or by uncouplers,  
 876 functioning like a clutch in a mechanical system. The corresponding coupling control state is  
 877 characterized by high levels of oxygen consumption without control by phosphorylation  
 878 ('uncontrolled state'). Energetic coupling is defined in **Box 4**. Loss of coupling lowers the  
 879 efficiency by intrinsic uncoupling and decoupling, or pathological dyscoupling. Such  
 880 generalized uncoupling is different from switching to mitochondrial pathways that involve  
 881 fewer than three proton pumps ('coupling sites': Complexes CI, CIII and CIV), bypassing CI  
 882 through multiple electron entries into the Q-junction (**Fig. 1**). A bypass of CIII and CIV is  
 883 provided by alternative oxidases, which reduce oxygen without proton translocation.  
 884 Reprogramming of mitochondrial pathways may be considered as a switch of gears (changing  
 885 the stoichiometry) rather than uncoupling (loosening the stoichiometry).

886 **Pathway control states** are obtained in mitochondrial preparations by depletion of  
 887 endogenous substrates and addition to the mitochondrial respiration medium of fuel substrates  
 888 (CHNO) and specific inhibitors, activating selected mitochondrial pathways (**Fig. 1**). Coupling  
 889 control states and pathway control states are complementary, since mitochondrial preparations  
 890 depend on an exogenous supply of pathway-specific fuel substrates and oxygen (Gnaiger 2014).  
 891

---

## 892 **Box 2: Metabolic fluxes and flows: vectorial and scalar**

893 In mitochondrial electron transfer (**Fig. 1**), vectorial transmembrane proton flux is coupled  
 894 through the proton pumps CI, CIII and CIV to the catabolic flux of scalar reactions, collectively  
 895 measured as oxygen flux. In **Fig. 2**, the scalar catabolic reaction,  $k$ , of oxygen consumption,  
 896  $J_{O_2,k}$  [ $\text{mol}\cdot\text{s}^{-1}\cdot\text{m}^{-3}$ ], is expressed as oxygen flux per volume,  $V$  [ $\text{m}^3$ ], of the instrumental chamber  
 897 (the system).

898 Fluxes are *vectors*, if they have *spatial* direction in addition to magnitude. A vector flux  
 899 (surface-density of flow) is expressed per unit cross-sectional area,  $A$  [ $\text{m}^2$ ], perpendicular to the  
 900 direction of flux. If *flows*,  $I$ , are defined as extensive quantities of the *system*, as vector or scalar  
 901 flow,  $\mathbf{I}$  or  $I$  [ $\text{mol}\cdot\text{s}^{-1}$ ], respectively, then the corresponding vector and scalar *fluxes*,  $\mathbf{J}$ , are  
 902 obtained as  $\mathbf{J} = \mathbf{I}\cdot A^{-1}$  [ $\text{mol}\cdot\text{s}^{-1}\cdot\text{m}^{-2}$ ] and  $J = I\cdot V^{-1}$  [ $\text{mol}\cdot\text{s}^{-1}\cdot\text{m}^{-3}$ ], respectively, expressing flux as an  
 903 area-specific vector or volume-specific scalar quantity.

904 Vectorial transmembrane proton fluxes,  $J_{H^+,pos}$  and  $J_{H^+,neg}$ , are analyzed in a heterogenous  
 905 compartmental system as a quantity with *directional* but not *spatial* information. Translocation  
 906 of protons across the mtIM has a defined direction, either from the negative compartment  
 907 (matrix space; negative, neg-compartment) to the positive compartment (inter-membrane  
 908 space; positive, pos-compartment) or *vice versa* (**Fig. 2**). The arrows defining the direction of  
 909 the translocation between the two compartments may point upwards or downwards, right or  
 910 left, without any implication that these are actual directions in space. The pos-compartment is  
 911 neither above nor below the neg-compartment in a spatial sense, but can be visualized arbitrarily  
 912 in a figure in the upper position (**Fig. 2**). In general, the *compartmental direction* of vectorial  
 913 translocation from the neg-compartment to the pos-compartment is defined by assigning the  
 914 initial and final state as *ergodynamic compartments*,  $H^+_{neg} \rightarrow H^+_{pos}$  or  $0 = -H^+_{neg} + H^+_{pos}$ , related  
 915 to work (erg = work) that must be performed to lift the proton from a lower to a higher  
 916 electrochemical potential or from the lower to the higher ergodynamic compartment (Gnaiger  
 917 1993b).

918 In direct analogy to *vectorial* translocation, the direction of a *scalar* chemical reaction,  $A$   
 919  $\rightarrow B$  or  $0 = -A+B$ , is defined by assigning substrates and products,  $A$  and  $B$ , as ergodynamic  
 920 compartments.  $O_2$  is defined as a substrate in respiratory  $O_2$  consumption, which together with  
 921 the fuel substrates comprises the substrate compartment of the catabolic reaction (**Fig. 2**).  
 922 Volume-specific scalar  $O_2$  flux is coupled (**Box 4**) to vectorial translocation. In order to  
 923 establish a quantitative relation between the coupled fluxes, both  $J_{O_2,k}$  and  $J_{H^+,pos}$  must be  
 924 expressed in identical units,  $[\text{mol}\cdot\text{s}^{-1}\cdot\text{m}^{-3}]$  or  $[\text{C}\cdot\text{s}^{-1}\cdot\text{m}^{-3}]$ , yielding the  $H^+_{pos}/O_2$  ratio (**Fig. 1**). The  
 925 *vectorial* proton flux in compartmental translocation has *compartmental direction*,  
 926 distinguished from a *vector* flux with *spatial direction*. Likewise, the corresponding  
 927 protonmotive force is defined as an electrochemical potential *difference* between two  
 928 compartments, in contrast to a *gradient* across the membrane or a vector force with defined  
 929 *spatial direction*.

---

930  
 931 **The steady-state:** Mitochondria represent a thermodynamically open system functioning  
 932 as a biochemical transformation system in non-equilibrium states. State variables (protonmotive  
 933 force; redox states) and metabolic fluxes (*rates*) are measured in defined mitochondrial  
 934 respiratory *states*. Strictly, steady states can be obtained only in open systems, in which changes  
 935 due to *internal* transformations, *e.g.*,  $O_2$  consumption, are instantaneously compensated for by  
 936 *external* fluxes *e.g.*,  $O_2$  supply, such that oxygen concentration does not change in the system  
 937 (Gnaiger 1993b). Mitochondrial respiratory states monitored in closed systems satisfy the  
 938 criteria of pseudo-steady states for limited periods of time, when changes in the system  
 939 (concentrations of  $O_2$ , fuel substrates, ADP,  $P_i$ ,  $H^+$ ) do not exert significant effects on metabolic  
 940 fluxes (respiration, phosphorylation). Such pseudo-steady states require respiratory media with  
 941 sufficient buffering capacity and kinetically-saturating concentrations of substrates to be  
 942 maintained, and thus depend on the kinetics of the processes under investigation. Proton  
 943 turnover,  $J_{\infty H^+}$ , and ATP turnover,  $J_{\infty P}$ , proceed in the steady-state at constant  $F_{H^+,pos}$ , when  $J_{H^+\infty}$   
 944  $= J_{H^+,pos} = J_{H^+,neg}$ , and at constant  $F_{P\gg}$ , when  $J_{P\infty} = J_{P\gg} = J_{P\ll}$  (**Fig. 2**).

### 945 3.3. Forces and fluxes in physics and thermodynamics

946  
 947 According to its definition in physics, a potential difference and as such the *protonmotive*  
 948 *force*,  $\Delta p$ , is not a force *per se* (Cohen *et al.* 2008). The fundamental forces of physics are  
 949 distinguished from *motive forces* of statistical and irreversible thermodynamics.  
 950 Complementary to the attempt towards unification of fundamental forces defined in physics,  
 951 the concepts of Nobel laureates Lars Onsager, Erwin Schrödinger, Ilya Prigogine and Peter  
 952 Mitchell unite (even if expressed in apparently unrelated terms) the diversity of *generalized* or  
 953 'isomorphic' *flux-force* relationships, the product of which links to entropy production and the  
 954 Second Law of thermodynamics (Schrödinger 1944; Prigogine 1967). A *motive force* is the  
 955 derivative of potentially available or 'free' energy (exergy) per *motive entity* (**Box 3**). Perhaps  
 956 the first account of a *motive force* in energy transformation can be traced back to the Peripatetic  
 957 school around 300 BC in the context of moving a lever, up to Newton's motive force  
 958 proportional to the alteration of motion (Coopersmith 2010). As a generalization, isomorphic  
 959 motive forces are considered as *entropic forces* in physics (Wang 2010).

---

### 962 **Box 3: Endergonic and exergonic transformations, exergy and dissipation**

963 A chemical reaction, or any transformation, is exergonic if the Gibbs energy change (exergy)  
 964 of the reaction is negative at constant temperature and pressure. The sum of Gibbs energy  
 965 changes of all internal transformations in a system can only be negative, *i.e.* exergy is  
 966 irreversibly dissipated. Endergonic reactions are characterized by positive Gibbs energies of  
 967 reaction and cannot proceed spontaneously in the forward direction as defined. For instance,

968 the endergonic reaction P» is coupled to exergonic catabolic reactions, such that the total Gibbs  
 969 energy change is negative, *i.e.* exergy must be dissipated for the reaction to proceed (**Fig. 2**).

970 In contrast, energy cannot be lost or produced in any internal process, which is the key  
 971 message of the First Law of thermodynamics. Thus mitochondria are the sites of energy  
 972 transformation but not energy production. Open and closed systems can gain energy and exergy  
 973 only by external fluxes, *i.e.* uptake from the environment. Exergy is the potential to perform  
 974 work. In the framework of flux-force relationships (**Box 4**), the *partial* derivative of Gibbs  
 975 energy per advancement of a transformation is an isomorphic force,  $F_{tr}$  (**Table 5**, Note 2). In  
 976 other words, force is equal to exergy per motive entity (in integral form, this definition takes  
 977 care of non-isothermal processes). This formal generalization represents an appreciation of the  
 978 conceptual beauty of Peter Mitchell's innovation of the protonmotive force against the  
 979 background of the established paradigm of the electromotive force (emf) defined at the limit of  
 980 zero current (Cohen *et al.* 2008).

---

981  
 982 **Vectorial and scalar forces, and fluxes:** In chemical reactions and osmotic or diffusion  
 983 processes occurring in a closed heterogeneous system, such as a chamber containing isolated  
 984 mitochondria, scalar transformations occur without measured spatial direction but between  
 985 separate compartments (displacement between the matrix and intermembrane space) or  
 986 between energetically-separated chemical substances (reactions from substrates to products).  
 987 Hence, the corresponding fluxes are not vectorial but scalar, and are expressed per volume and  
 988 not per membrane area (**Box 2**). The corresponding motive forces are also scalar potential  
 989 *differences* across the membrane (**Table 5**), without taking into account the *gradients* across  
 990 the 6 nm thick mtIM (Rich 2003).

991 **Coupling:** In energetics (ergodynamics), coupling is defined as an energy transformation  
 992 fuelled by an exergonic (downhill) input process driving the advancement of an endergonic  
 993 (uphill) output process. The (negative) output/input power ratio is the efficiency of a coupled  
 994 energy transformation (**Box 4**). At the limit of maximum efficiency of a completely coupled  
 995 system, the (negative) input power equals the (positive) output power, such that the total power  
 996 approaches zero at the maximum efficiency of 1, and the process becomes fully reversible  
 997 without any dissipation of exergy, *i.e.* without entropy production.

998

---

#### 999 **Box 4: Coupling, power and efficiency, at constant temperature and pressure**

1000 Energetic coupling means that two processes of energy transformation are linked such that the  
 1001 input power,  $P_{in}$ , is the driving element of the output power,  $P_{out}$ , and the (negative) out/input  
 1002 power ratio is the efficiency. In general, power is work per unit time [ $J \cdot s^{-1} = W$ ]. When  
 1003 describing a system with volume  $V$  without information on the internal structure, the output is  
 1004 defined as the *external* work (exergy) performed by the *total* system on its environment. Such  
 1005 a system may be open for any type of exchange, or closed and thus allowing only heat and work  
 1006 to be exchanged across the system boundaries. This is the classical black box approach of  
 1007 thermodynamics. In contrast, in a colourful compartmental analysis of *internal* energy  
 1008 transformations (**Fig. 2**), the system is structured and described by definition of ergodynamic  
 1009 compartments (with information on the heterogeneity of the system; **Box 2**) and analysis of  
 1010 separate parts, *i.e.* a sequence of *partial* energy transformations, tr. At constant temperature and  
 1011 pressure, power per unit volume,  $P_{V,tr} = P_{tr}/V$  [ $W \cdot m^{-3}$ ], is the product of a volume-specific flux,  
 1012  $J_{tr}$ , and its conjugated force,  $F_{tr}$ , and is directly linked to entropy production,  $d_i S/dt = \sum_{tr} P_{tr}/T$   
 1013 [ $W \cdot K^{-1}$ ], as generalized by irreversible thermodynamics (Prigogine 1967; Gnaiger 1993a,b).  
 1014 Output power of proton translocation and catabolic input power are (**Fig. 2**),

1015 Output:  $P_{H^+,pos}/V = J_{H^+,pos} \cdot F_{H^+,pos}$   
 1016 Input:  $P_k/V = J_{O_2,k} \cdot F_{O_2,k}$

1017  $F_{O_2,k}$  is the exergonic input force with a negative sign, and,  $F_{H^+,pos}$ , is the endergonic output  
 1018 force with a positive sign (**Box 3**). Ergodynamic efficiency is the ratio of output/input power,  
 1019 or the flux ratio times force ratio (Gnaiger 1993a,b),

$$1020 \quad \varepsilon = \frac{P_{H^+,pos}}{-P_k} = \frac{J_{H^+,pos}}{J_{O_2,k}} \cdot \frac{F_{H^+,pos}}{-F_{O_2,k}}$$

1021 The concept of incomplete coupling relates exclusively to the first term, *i.e.* the flux ratio, or  
 1022  $H^+_{pos}/O_2$  ratio (**Fig. 1**). Likewise, respirometric definitions of the  $P_{\gg}/O_2$  ratio and biochemical  
 1023 coupling efficiency (Section 3.2) consider flux ratios. In a completely coupled process, the  
 1024 power efficiency,  $\varepsilon$ , depends entirely on the force ratio, ranging from zero efficiency at an  
 1025 output force of zero, to the limiting output force and maximum efficiency of 1.0, when the total  
 1026 power of the coupled process,  $P_t = P_k + P_{H^+,pos}$ , equals zero, and any net flows are zero at  
 1027 ergodynamic equilibrium of a coupled process. Thermodynamic equilibrium is defined as the  
 1028 state when all potentials (all forces) are dissipated and equilibrate towards their minima of zero.  
 1029 In a fully or completely coupled process, output and input fluxes are directly proportional in a  
 1030 fixed ratio technically defined as a stoichiometric relationship (a gear ratio in a mechanical  
 1031 system). Such maximal stoichiometric output/input flux ratios are considered in OXPPOS  
 1032 analysis as the upper limits or mechanistic  $H^+_{pos}/O_2$  and  $P_{\gg}/O_2$  ratios (**Fig. 1**).

---

1033  
 1034 **Coupled versus bound processes:** Since the chemiosmotic theory describes the  
 1035 mechanisms of coupling in OXPPOS, it may be interesting to ask if the electrical and chemical  
 1036 parts of proton translocation are coupled processes. This is not the case according to the  
 1037 definition of coupling. If the coupling mechanism is disengaged, the output process becomes  
 1038 independent of the input process, and both proceed in their downhill (exergonic) direction (**Fig.**  
 1039 **2**). It is not possible to physically uncouple the electrical and chemical processes, which are  
 1040 only *theoretically* partitioned as electrical and chemical components. The electrical and  
 1041 chemical partial protonmotive *forces*,  $F_{el,pos}$  and  $F_{H^+,pos,d}$ , can be measured separately. In  
 1042 contrast, the corresponding proton *flux*,  $J_{H^+,pos}$ , is non-separable, *i.e.*, cannot be uncoupled. Then  
 1043 these are not *coupled* processes, but are defined as *bound* processes. The electrical and chemical  
 1044 parts are tightly bound partial forces, since the flux cannot be partitioned but expressed only in  
 1045 either an electrical or chemical format,  $J_{H^+/e}$  or  $J_{H^+/n}$  (**Table 4**).

#### 1046 1047 **4. Normalization: fluxes and flows**

1048  
 1049 The challenges of measuring mitochondrial respiratory flux are matched by those of  
 1050 normalization, whereby  $O_2$  consumption may be considered as the numerator and normalization  
 1051 as the complementary denominator, which are tightly linked in reporting the measurements in  
 1052 a format commensurate with the requirements of a database.

##### 1053 1054 *4.1. Flux per chamber volume*

1055  
 1056 When the reactor volume does not change during the reaction, which is typical for liquid  
 1057 phase reactions, the volume-specific *flux of a chemical reaction*  $r$  is the time derivative of the  
 1058 advancement of the reaction per unit volume,  $J_{V,B} = d\zeta_B/dt \cdot V^{-1}$  [(mol·s<sup>-1</sup>)·L<sup>-1</sup>]. The *rate of*  
 1059 *concentration change* is  $dc_B/dt$  [(mol·L<sup>-1</sup>)·s<sup>-1</sup>], where concentration is  $c_B = n_B/V$ . It is helpful to  
 1060 make the subtle distinction between [(mol·s<sup>-1</sup>)·L<sup>-1</sup>] and [mol·L<sup>-1</sup>·s<sup>-1</sup>] for the fundamentally  
 1061 different quantities of volume-specific flux and rate of concentration change, which merge to a  
 1062 single expression only in closed systems. In open systems, external fluxes (such as  $O_2$  supply)  
 1063 are distinguished from internal transformations (metabolic flux,  $O_2$  consumption). In a closed  
 1064 system, external flows of all substances are zero and  $O_2$  consumption (internal flow),  $I_{O_2}$   
 1065 [pmol·s<sup>-1</sup>], causes a decline of the amount of  $O_2$  in the system,  $n_{O_2}$  [nmol]. Normalization of  
 1066 these quantities for the volume of the system,  $V$  [L = dm<sup>3</sup>], yields volume-specific  $O_2$  flux,  $J_{V,O_2}$



1067  $= I_{O_2}/V$  [ $\text{nmol}\cdot\text{s}^{-1}\cdot\text{L}^{-1}$ ], and  $O_2$  concentration,  $[O_2]$  or  $c_{O_2} = n_{O_2}/V$  [ $\mu\text{mol}\cdot\text{L}^{-1} = \mu\text{M} = \text{nmol}\cdot\text{mL}^{-1}$ ].  
 1068 Instrumental background  $O_2$  flux is due to external flux into a non-ideal closed respirometer,  
 1069 such that total volume-specific flux has to be corrected for instrumental background  $O_2$  flux,  
 1070 *i.e.*  $O_2$  diffusion into or out of the instrumental chamber.  $J_{V,O_2}$  is relevant mainly for  
 1071 methodological reasons and should be compared with the accuracy of instrumental resolution  
 1072 of background-corrected flux, *e.g.*  $\pm 1 \text{ nmol}\cdot\text{s}^{-1}\cdot\text{L}^{-1}$  (Gnaiger 2001). ‘Metabolic’ or catabolic  
 1073 indicates  $O_2$  flux,  $J_{O_2,k}$ , corrected for instrumental background  $O_2$  flux and chemical background  
 1074  $O_2$  flux due to autoxidation of chemical components added to the incubation medium.

1075

#### 1076 4.2. System-specific and sample-specific normalization

1077

1078 Application of common and generally defined units is required for direct transfer of  
 1079 reported results into a database. The second [s] is the *SI* unit for the base quantity *time*. It is also  
 1080 the standard time-unit used in solution chemical kinetics. **Table 6** lists some conversion factors  
 1081 to obtain *SI* units. The term *rate* is not sufficiently defined to be useful for a database (**Fig. 8**).  
 1082 The inconsistency of the meanings of rate becomes fully apparent when considering Galileo  
 1083 Galilei’s famous principle, that ‘bodies of different weight all fall at the same rate (have a  
 1084 constant acceleration)’ (Coopersmith 2010).

1085

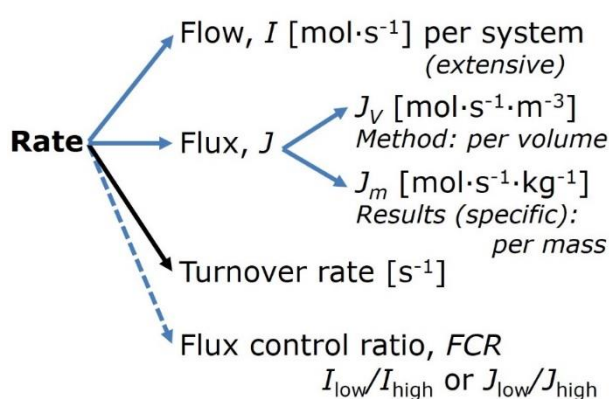
1086 **Fig. 8. Different meanings of rate may lead to confusion, if the normalization is not**  
 1087 **sufficiently specified.** Results are frequently  
 1088 expressed as mass-specific flux,  $J_m$ , per mg  
 1089 protein, dry or wet weight (mass). Cell  
 1090 volume,  $V_{\text{cell}}$ , or mitochondrial volume,  $V_{\text{mt}}$ ,  
 1091 may be used for normalization (volume-  
 1092 specific flux,  $J_{V_{\text{cell}}}$  or  $J_{V_{\text{mt}}}$ ), which then must  
 1093 be clearly distinguished from flux,  $J_V$ ,  
 1094 expressed for methodological reasons per  
 1095 volume of the measurement system, or flow  
 1096 per cell,  $I_X$ .

1098

1099 **Extensive quantities:** An extensive quantity increases proportionally with system size.  
 1100 The magnitude of an extensive quantity is completely additive for non-interacting subsystems,  
 1101 such as mass or flow expressed per defined system. The magnitude of these quantities depends  
 1102 on the extent or size of the system (Cohen *et al.* 2008).

1103 **Size-specific quantities:** ‘The adjective *specific* before the name of an extensive quantity  
 1104 is often used to mean *divided by mass*’ (Cohen *et al.* 2008). Mass-specific flux is flow divided  
 1105 by mass of the system. A mass-specific quantity is independent of the extent of non-interacting  
 1106 homogenous subsystems. Tissue-specific quantities are of fundamental interest in comparative  
 1107 mitochondrial physiology, where *specific* refers to the *type* rather than *mass* of the tissue. The  
 1108 term *specific*, therefore, must be further clarified, such that tissue mass-specific, *e.g.*, muscle  
 1109 mass-specific quantities are defined.

1110 **Molar quantities:** ‘The adjective *molar* before the name of an extensive quantity  
 1111 generally means *divided by amount of substance*’ (Cohen *et al.* 2008). The notion that all molar  
 1112 quantities then become *intensive* causes ambiguity in the meaning of *molar Gibbs energy*. It is  
 1113 important to emphasize the fundamental difference between normalization for amount of  
 1114 substance *in a system* or for amount of motive substance *in a transformation*. When the Gibbs  
 1115 energy of a system,  $G$  [J], is divided by the amount of substance B in the system,  $n_B$  [mol], a  
 1116 *size-specific* molar quantity is obtained,  $G_B = G/n_B$  [ $\text{J}\cdot\text{mol}^{-1}$ ], which is not any force at all. In  
 1117 contrast, when the partial Gibbs energy change,  $\partial G$  [J], is divided by the motive amount of



1118 substance B in reaction r (advancement of reaction),  $\partial_r \xi_B$  [mol], the resulting intensive molar  
 1119 quantity,  $F_{B,r} = \partial G / \partial r \xi_B$  [J·mol<sup>-1</sup>], is the chemical motive force of reaction r involving 1 mol B  
 1120 (**Table 5**, Note 4).

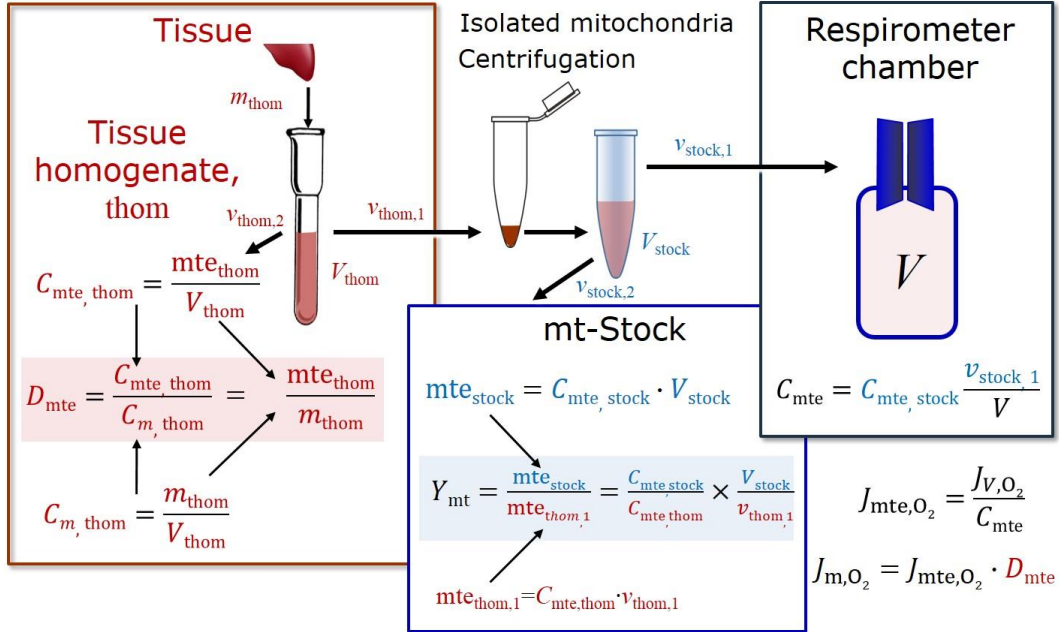
1121 **Flow per system,  $I$ :** In analogy to electrical terms, flow as an extensive quantity ( $I$ ; per  
 1122 system) is distinguished from flux as a size-specific quantity ( $J$ ; per system size) (**Fig. 8**).  
 1123 Electric current is flow,  $I_{el}$  [A = C·s<sup>-1</sup>] per system (extensive quantity). When dividing this  
 1124 extensive quantity by system size (membrane area), a size-specific quantity is obtained, which  
 1125 is electric flux (electric current density),  $J_{el}$  [A·m<sup>-2</sup> = C·s<sup>-1</sup>·m<sup>-2</sup>].  
 1126

1127 **Table 6. Sample concentrations and normalization of flux with SI/base units.**  
 1128

Expression	Symbol	Definition	SI Unit	Notes
<b>Sample</b>				
Identity of sample	$X$	Cells, animals, patients		
Number of sample entities $X$	$N_X$	Number of cells, <i>etc.</i>	x	
Mass of sample $X$	$m_X$		kg	1
Mass of entity $X$	$M_X$	$M_X = m_X \cdot N_X^{-1}$	kg·x <sup>-1</sup>	1
<b>Mitochondria</b>				
Mitochondria	mt	$X = mt$		
Amount of mt-elements	mte	Quantity of mt-marker	$x_{mte}$	
<b>Concentrations</b>				
Sample number concentration	$C_{NX}$	$C_{NX} = N_X \cdot V^{-1}$	x·m <sup>-3</sup>	2
Sample mass concentration	$C_{mX}$	$C_{mX} = m_X \cdot V^{-1}$	kg·m <sup>-3</sup>	
Mitochondrial concentration	$C_{mte}$	$C_{mte} = mte \cdot V^{-1}$	$x_{mte} \cdot m^{-3}$	3
Specific mitochondrial density	$D_{mte}$	$D_{mte} = mte \cdot m_X^{-1}$	$x_{mte} \cdot kg^{-1}$	4
Mitochondrial content, mte per entity $X$	$mte_X$	$mte_X = mte \cdot N_X^{-1}$	$x_{mte} \cdot x^{-1}$	5
<b>O<sub>2</sub> flow and flux</b>				
Flow	$I_{O_2}$	Internal flow	mol·s <sup>-1</sup>	6
Volume-specific flux	$J_{V,O_2}$	$J_{V,O_2} = I_{O_2} \cdot V^{-1}$	mol·s <sup>-1</sup> ·m <sup>-3</sup>	7
Flow per sample entity $X$	$I_{X,O_2}$	$I_{X,O_2} = J_{V,O_2} \cdot C_{NX}^{-1}$	mol·s <sup>-1</sup> ·x <sup>-1</sup>	8
Mass-specific flux	$J_{mX,O_2}$	$J_{mX,O_2} = J_{V,O_2} \cdot C_{mX}^{-1}$	mol·s <sup>-1</sup> ·kg <sup>-1</sup>	9
Mitochondria-specific flux	$J_{mte,O_2}$	$J_{mte,O_2} = J_{V,O_2} \cdot C_{mte}^{-1}$	mol·s <sup>-1</sup> · $x_{mte}^{-1}$	10

- 1129  
 1130 1 The SI prefix k is used for the SI base unit of mass (kg = 1,000 g). In praxis, various SI prefixes are  
 1131 used for convenience, to make numbers easily readable, e.g. 1 mg tissue, cell or mitochondrial mass  
 1132 instead of 0.000001 kg.  
 1133 2 In case  $X = \text{cells}$ , the sample number concentration is  $C_{N_{cell}} = N_{cell} \cdot V^{-1}$ , and volume may be expressed  
 1134 in [dm<sup>3</sup> = L] or [cm<sup>3</sup> = mL]. See **Table 7** for different sample types.  
 1135 3 mt-concentration is an experimental variable, dependent on sample concentration: (1)  $C_{mte} = mte \cdot V^{-1}$ ;  
 1136 (2)  $C_{mte} = mte_X \cdot C_{NX}$ ; (3)  $C_{mte} = C_{mX} \cdot D_{mte}$ .  
 1137 4 If the amount of mitochondria, mte, is expressed as mitochondrial mass, then  $D_{mte}$  is the mass  
 1138 fraction of mitochondria in the sample. If mte is expressed as mitochondrial volume,  $V_{mt}$ , and the  
 1139 mass of sample,  $m_X$ , is replaced by volume of sample,  $V_X$ , then  $D_{mte}$  is the volume fraction of  
 1140 mitochondria in the sample.  
 1141 5  $mte_X = mte \cdot N_X^{-1} = C_{mte} \cdot C_{NX}^{-1}$ .  
 1142 6 O<sub>2</sub> can be replaced by other chemicals B to study different reactions, e.g. ATP, H<sub>2</sub>O<sub>2</sub>, or  
 1143 compartmental translocations, e.g. Ca<sup>2+</sup>.  
 1144 7  $I_{O_2}$  and  $V$  are defined per instrument chamber as a system of constant volume (and constant  
 1145 temperature), which may be closed or open.  $I_{O_2}$  is abbreviated for  $I_{O_2,r}$ , i.e. the metabolic or internal

- 1146  $O_2$  flow of the chemical reaction  $r$  in which  $O_2$  is consumed, hence the negative stoichiometric  
 1147 number,  $\nu_{O_2} = -1$ .  $I_{O_2,r} = d_r n_{O_2} / dt \cdot \nu_{O_2}^{-1}$ . If  $r$  includes all chemical reactions in which  $O_2$  participates, then  
 1148  $d_r n_{O_2} = dn_{O_2} - d_e n_{O_2}$ , where  $dn_{O_2}$  is the change in the amount of  $O_2$  in the instrument chamber and  $d_e n_{O_2}$   
 1149 is the amount of  $O_2$  added externally to the system. At steady state, by definition  $dn_{O_2} = 0$ , hence  $d_r n_{O_2}$   
 1150  $= -d_e n_{O_2}$ .
- 1151 8  $J_{V,O_2}$  is an experimental variable, expressed per volume of the instrument chamber.  
 1152 9  $I_{X,O_2}$  is a physiological variable, depending on the size of entity  $X$ .  
 1153 10 There are many ways to normalize for a mitochondrial marker, that are used in different experimental  
 1154 approaches: (1)  $J_{mte,O_2} = J_{V,O_2} \cdot C_{mte}^{-1}$ ; (2)  $J_{mte,O_2} = J_{V,O_2} \cdot C_m^{-1} \cdot D_{mte}^{-1} = J_{mX,O_2} \cdot D_{mte}^{-1}$ ; (3)  $J_{mte,O_2} = J_{V,O_2} \cdot C_{NX}^{-1} \cdot mte_X^{-1}$   
 1155  $= I_{X,O_2} \cdot mte_X^{-1}$ ; (4)  $J_{mte,O_2} = I_{O_2} \cdot mte^{-1}$ .  
 1156  
 1157



1158

Symbol	Definition [Units]
$C_{mte}$	Mitochondrial concentration in chamber [ $x_{mte} \cdot L^{-1}$ ]
$C_m$	Sample mass concentration in chamber [ $g \cdot L^{-1}$ ]
$D_{mte}$	Specific mte-density per tissue mass [ $x_{mte} \cdot g^{-1}$ ]
$J_{m, O_2}$	Mass-specific $O_2$ flux [ $nmol \cdot s^{-1} \cdot g^{-1}$ ]
$J_{mte, O_2}$	Mitochondria-specific $O_2$ flux [ $nmol \cdot s^{-1} \cdot x_{mte}^{-1}$ ]
$mte$	Amount of mitochondrial elements [ $x_{mte}$ ]
$m_{thom}$	Mass of tissue in the homogenate [g]
$Y_{mt}$	Yield of isolated mitochondria

**Respirometer chamber**

**Homogenate**

$v_{thom,1}$

$V$

$C_m = C_{m, thom} \frac{v_{thom,1}}{V}$

$C_{mte} = C_m \cdot D_{mte}$

$J_{m, O_2} = \frac{J_{V, O_2}}{C_m}$

$J_{mte, O_2} = \frac{J_{m, O_2}}{D_{mte}}$

1160

1161

1162

1163

1164

1165

1166

1167

1168

**Fig. 9. Normalization of volume-specific flux of isolated mitochondria and tissue homogenate. A:** Mitochondrial yield,  $Y_{mt}$ , in preparation of isolated mitochondria.  $v_{thom,1}$  and  $v_{stock,1}$  are the volumes transferred from the total volume,  $V_{thom}$  and  $V_{stock}$ , respectively.  $mte_{thom,1}$  is the amount of mitochondrial elements in volume  $v_{thom,1}$  used for isolation. **B:** In respirometry with homogenate,  $v_{thom,1}$  is transferred directly into the respirometer chamber. See **Table 6** for further explanation of symbols.

1169

**Table 7. Some useful abbreviations of various sample types, X.**

Identity of sample	X
Mitochondrial preparation	mtprep
Isolated mitochondria	imt
Tissue homogenate	thom
Permeabilized tissue	pti
Permeabilized fibre	pfi
Permeabilized cell	pce
Cell	ce
Organism	org

1170

1171 **Size-specific flux, J:** Metabolic O<sub>2</sub> flow per tissue increases as tissue mass is increased.

1172 Tissue mass-specific O<sub>2</sub> flux should be independent of the size of the tissue sample studied in  
 1173 the instrument chamber, but volume-specific O<sub>2</sub> flux (per volume of the instrument chamber,  
 1174 V) should increase in direct proportion to the amount of sample in the chamber. Accurate  
 1175 definition of the experimental system is decisive: whether the experimental chamber is the  
 1176 closed, open, isothermal or non-isothermal *system* with defined volume as part of the  
 1177 measurement apparatus, in contrast to the experimental *sample* in the chamber (**Table 6**).  
 1178 Volume-specific O<sub>2</sub> flux depends on mass-concentration of the sample in the chamber, but  
 1179 should be independent of the chamber volume. There are practical limitations to increasing the  
 1180 mass-concentration of the sample in the chamber, when one is concerned about crowding  
 1181 effects and instrumental time resolution.

1182 **Sample concentration C<sub>mX</sub>:** Normalization for sample concentration is required for  
 1183 reporting respiratory data. Consider a tissue or cells as the sample, X, and the sample mass, m<sub>X</sub>  
 1184 [mg] from which a mitochondrial preparation is obtained. m<sub>X</sub> is frequently measured as wet or  
 1185 dry weight, W<sub>w</sub> or W<sub>d</sub> [mg], or as amount of tissue or cell protein, m<sub>Protein</sub>. In the case of  
 1186 permeabilized tissues, cells, and homogenates, the sample concentration, C<sub>mX</sub> = m<sub>X</sub>/V [mg·mL<sup>-1</sup>  
 1187 = g·L<sup>-1</sup>], is simply the mass of the subsample of tissue that is transferred into the instrument  
 1188 chamber. Part of the mitochondria from the tissue is lost during preparation of isolated  
 1189 mitochondria. The fraction of mitochondria obtained is expressed as mitochondrial yield (**Fig.**  
 1190 **9**). At a high mitochondrial yield the sample of isolated mitochondria is more representative of  
 1191 the total mitochondrial population than in preparations characterized by low mitochondrial  
 1192 yield. Determination of the mitochondrial yield is based on measurement of the concentration  
 1193 of a mitochondrial marker in the tissue homogenate, C<sub>mtc,thom</sub>, which simultaneously provides  
 1194 information on the specific mitochondrial density in the sample (**Fig. 9**).

1195 Tissues can contain multiple cell populations which may have distinct mitochondrial  
 1196 subtypes. Mitochondria undergo dynamic fission and fusion cycles, and can exist in multiple  
 1197 stages and sizes which may be altered by a range of factors. The isolation of mitochondria (often  
 1198 achieved through differential centrifugation) can therefore yield a subsample of the  
 1199 mitochondrial types present in a tissue, dependent on isolation protocols utilized (*e.g.*  
 1200 centrifugation speed). This possible artefact should be taken into account when planning  
 1201 experiments using isolated mitochondria. The tendency for mitochondria of specific sizes to be  
 1202 enriched at different centrifugation speeds also has the potential to allow the isolation of specific  
 1203 mitochondrial subpopulations and therefore the analysis of mitochondria from multiple cell  
 1204 lineages within a single tissue.

1205 **Mass-specific flux, J<sub>mX,O<sub>2</sub></sub>:** Mass-specific flux is obtained by expressing respiration per  
 1206 mass of sample, m<sub>X</sub> [mg]. X is the type of sample, *e.g.*, tissue homogenate, permeabilized fibres  
 1207 or cells. Volume-specific flux is divided by mass concentration of X, J<sub>mX,O<sub>2</sub></sub> = J<sub>V,O<sub>2</sub></sub>/C<sub>mX</sub>; or flow  
 1208 per cell is divided by mass per cell, J<sub>mcell,O<sub>2</sub></sub> = I<sub>cell,O<sub>2</sub></sub>/M<sub>cell</sub>. If mass-specific O<sub>2</sub> flux is constant  
 1209 and independent of sample size (expressed as mass), then there is no interaction between the  
 1210 subsystems. A 1.5 mg and a 3.0 mg muscle sample respire at identical mass-specific flux.

1211 Mass-specific O<sub>2</sub> flux, however, may change with the mass of a tissue sample, cells or isolated  
 1212 mitochondria in the measuring chamber, in which case the nature of the interaction becomes an  
 1213 issue. Optimization of cell density and arrangement is generally important and particularly in  
 1214 experiments carried out in wells, considering the confluency of the cell monolayer or clumps  
 1215 of cells (Salabei *et al.* 2014).

1216 **Number concentration,  $C_{NX}$ :**  $C_{NX}$  is the experimental *number concentration* of sample  
 1217 in the case of cells or animals, *e.g.*, nematodes is  $C_{NX} = N_X/V$  [ $x \cdot L^{-1}$ ], where  $N_X$  is the number  
 1218 of cells or organisms in the chamber (**Table 6**).

1219 **Flow per sample entity,  $I_{X,O_2}$ :** A special case of normalization is encountered in  
 1220 respiratory studies with permeabilized (or intact) cells. If respiration is expressed per cell, the  
 1221 O<sub>2</sub> flow per measurement system is replaced by the O<sub>2</sub> flow per cell,  $I_{cell,O_2}$  (**Table 6**). O<sub>2</sub> flow  
 1222 can be calculated from volume-specific O<sub>2</sub> flux,  $J_{V,O_2}$  [ $nmol \cdot s^{-1} \cdot L^{-1}$ ] (per  $V$  of the measurement  
 1223 chamber [L]), divided by the number concentration of cells,  $C_{Nce} = N_{ce}/V$  [ $cell \cdot L^{-1}$ ], where  $N_{ce}$   
 1224 is the number of cells in the chamber. Cellular O<sub>2</sub> flow can be compared between cells of  
 1225 identical size. To take into account changes and differences in cell size, further normalization  
 1226 is required to obtain cell size-specific or mitochondrial marker-specific O<sub>2</sub> flux (Renner *et al.*  
 1227 2003).

1228 The complexity changes when the sample is a whole organism studied as an experimental  
 1229 model. The well-established scaling law in respiratory physiology reveals a strong interaction  
 1230 of O<sub>2</sub> consumption and individual body mass of an organism, since *basal* metabolic rate (flow)  
 1231 does not increase linearly with body mass, whereas *maximum* mass-specific O<sub>2</sub> flux,  $\dot{V}_{O_{2max}}$  or  
 1232  $\dot{V}_{O_{2peak}}$ , is approximately constant across a large range of individual body mass (Weibel and  
 1233 Hoppeler 2005), with individuals, breeds, and certain species deviating substantially from this  
 1234 general relationship.  $\dot{V}_{O_{2peak}}$  of human endurance athletes is 60 to 80 mL O<sub>2</sub> · min<sup>-1</sup> · kg<sup>-1</sup> body  
 1235 mass, converted to  $J_{m,O_{2peak}}$  of 45 to 60 nmol · s<sup>-1</sup> · g<sup>-1</sup> (Gnaiger 2014; **Table 8**).

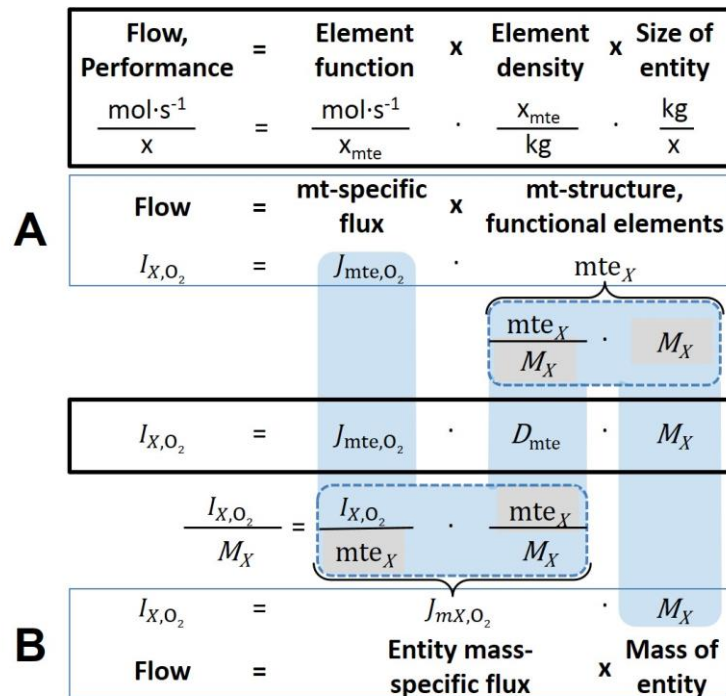
#### 1237 4.3. Normalization for mitochondrial content

1238  
 1239 Normalization is a problematic subject and it is essential to consider the question of the  
 1240 study. If the study aims to compare tissue performance, such as the effects of a certain treatment  
 1241 on a specific tissue, then normalization can be successful, using tissue mass or protein content,  
 1242 for example. If the aim, however, is to find differences of mitochondrial function independent  
 1243 of mitochondrial density (**Table 6**), then normalization to a mitochondrial marker is imperative  
 1244 (**Fig. 10**). However, one cannot assume that quantitative changes in various markers such as  
 1245 mitochondrial proteins necessarily occur in parallel with one another. It is important to first  
 1246 establish that the marker chosen is not selectively altered by the performed treatment. In  
 1247 conclusion, the normalization must reflect the question under investigation to reach a satisfying  
 1248 answer. On the other hand, the goal of comparing results across projects and institutions  
 1249 requires some standardization on normalization for entry into a databank.

1250 **Mitochondrial concentration,  $C_{mte}$ , and mitochondrial markers:** It is important that  
 1251 mitochondrial concentration in the tissue and the measurement chamber be quantified, as a  
 1252 physiological output and result of mitochondrial biogenesis and degradation, and as a quantity  
 1253 for normalization in functional analyses. Mitochondrial organelles comprise a dynamic cellular  
 1254 reticulum in various states of fusion and fission. Hence the definition of an "amount" of  
 1255 mitochondria is often misconceived: mitochondria cannot be counted as a number of occurring  
 1256 elements. Therefore, quantification of the "amount" of mitochondria depends on measurement  
 1257 of chosen mitochondrial markers. 'Mitochondria are the structural and functional elemental  
 1258 units of cell respiration' (Gnaiger 2014). The quantity of a mitochondrial marker can be  
 1259 considered to reflect the amount of *elemental mitochondrial units* or *mitochondrial elements*,  
 1260 mte. However, since mitochondrial quality changes under certain stimuli, particularly in  
 1261 mitochondrial dysfunction and after exercise training (Pesta *et al.* 2011; Campos *et al.* 2017),

1262 some markers can vary while other markers are unchanged: (1) Mitochondrial volume and  
 1263 membrane area are structural markers, whereas mitochondrial protein mass is frequently used  
 1264 as a marker for isolated mitochondria. (2) Molecular and enzymatic mitochondrial markers  
 1265 (amounts or activities) can be selected as matrix markers, *e.g.*, citrate synthase activity, mtDNA;  
 1266 mtIM-markers, *e.g.*, cytochrome *c* oxidase activity, *aa*<sub>3</sub> content, cardiolipin, or mtOM-markers,  
 1267 *e.g.*, TOM20. (3) Extending the measurement of mitochondrial marker enzyme activity to  
 1268 mitochondrial pathway capacity, measured as ET- or OXPHOS-capacity, can be considered as  
 1269 an integrative functional mitochondrial marker.

1270 Depending on the type of mitochondrial marker, the mitochondrial elements, *mte*, are  
 1271 expressed in marker-specific units. Although concentration and density are used synonymously  
 1272 in physical chemistry, it is recommended to distinguish *experimental mitochondrial*  
 1273 *concentration*,  $C_{mte} = mte/V$  and *physiological mitochondrial density*,  $D_{mte} = mte/m_X$ . Then  
 1274 mitochondrial density is the amount of mitochondrial elements per mass of tissue (Fig. 10). The  
 1275 former is mitochondrial density multiplied by sample mass concentration,  $C_{mte} = D_{mte} \cdot C_{mX}$ , or  
 1276 mitochondrial content multiplied by sample number concentration,  $C_{mte} = mte_X \cdot C_{NX}$  (Table 6).  
 1277



1278 **Fig. 10. Structure-function analysis of performance of an organism, organ or tissue, or a**  
 1279 **cell (sample entity  $X$ ).  $O_2$  flow,  $I_{X,O_2}$ , is the product of performance per functional element**  
 1280 **(element function, mitochondria-specific flux), element density (mitochondrial density,**  
 1281  **$D_{mte}$ ), and size of entity  $X$  (mass  $M_X$ ). (A) Structured analysis: performance is the product of**  
 1282 **mitochondrial *function* (mt-specific flux) and *structure* (functional elements;  $D_{mte}$  times mass**  
 1283 **of  $X$ ). (B) Unstructured analysis: performance is the product of *entity mass-specific flux*,  $J_{mX,O_2}$**   
 1284  **$= I_{X,O_2}/M_X = I_{O_2}/m_X$  [ $\text{mol} \cdot \text{s}^{-1} \cdot \text{kg}^{-1}$ ] and *size of entity*, expressed as mass of  $X$ ;  $M_X = m_X \cdot N_X^{-1}$**   
 1285  **$[\text{kg} \cdot \text{x}^{-1}]$ . See Table 6 for further explanation of quantities and units. Modified from Gnaiger**  
 1286 **(2014).**

1287  
 1288  
 1289 **Mitochondria-specific flux,  $J_{mte,O_2}$ :** Volume-specific metabolic  $O_2$  flux depends on: (1)  
 1290 the sample concentration in the volume of the instrument chamber,  $C_{mX}$ , or  $C_{NX}$ ; (2) the  
 1291 mitochondrial density in the sample,  $D_{mte} = mte/m_X$  or  $mte_X = mte/N_X$ ; and (3) the specific  
 1292 mitochondrial activity or performance per elemental mitochondrial unit,  $J_{mte,O_2} = J_{V,O_2}/C_{mte}$   
 1293 (Table 6). Obviously, the numerical results for  $J_{mte,O_2}$  vary according to the type of  
 1294 mitochondrial marker chosen for measurement of *mte* and  $C_{mte} = mte/V$ .

#### 1295 4.4. Evaluation of mitochondrial markers

1296  
 1297 Different methods are implicated in quantification of mitochondrial markers and have  
 1298 different strengths. Some problems are common for all mitochondrial markers, mte: (1)  
 1299 Accuracy of measurement is crucial, since even a highly accurate and reproducible  
 1300 measurement of O<sub>2</sub> flux results in an inaccurate and noisy expression normalized for a biased  
 1301 and noisy measurement of a mitochondrial marker. This problem is acute in mitochondrial  
 1302 respiration because the denominators used (the mitochondrial markers) are often very small  
 1303 moieties whose accurate and precise determination is difficult. This problem can be avoided  
 1304 when O<sub>2</sub> fluxes measured in substrate-uncoupler-inhibitor titration protocols are normalized for  
 1305 flux in a defined respiratory reference state, which is used as an *internal* marker and yields flux  
 1306 control ratios, *FCRs* (Fig. 8). *FCRs* are independent of any *externally* measured markers and,  
 1307 therefore, are statistically very robust, considering the limitations of ratios in general (Jasienski  
 1308 and Bazzaz 1999). *FCRs* indicate qualitative changes of mitochondrial respiratory control, with  
 1309 highest quantitative resolution, separating the effect of mitochondrial density or concentration  
 1310 on  $J_{mX,O_2}$  and  $I_{X,O_2}$  from that of function per elemental mitochondrial marker,  $J_{mte,O_2}$  (Pesta *et al.*  
 1311 2011; Gnaiger 2014). (2) If mitochondrial quality does not change and only the amount of  
 1312 mitochondria varies as a determinant of mass-specific flux, any marker is equally qualified in  
 1313 principle; then in practice selection of the optimum marker depends only on the accuracy and  
 1314 precision of measurement of the mitochondrial marker. (3) If mitochondrial flux control ratios  
 1315 change, then there may not be any best mitochondrial marker. In general, measurement of  
 1316 multiple mitochondrial markers enables a comparison and evaluation of normalization for a  
 1317 variety of mitochondrial markers. Particularly during postnatal development, the activity of  
 1318 marker enzymes, such as cytochrome *c* oxidase and citrate synthase, follows different time  
 1319 courses (Drahota *et al.* 2004). Evaluation of mitochondrial markers in healthy controls is  
 1320 insufficient for providing guidelines for application in the diagnosis of pathological states and  
 1321 specific treatments.

1322 In line with the concept of the respiratory control ratio (Chance and Williams 1955a), the  
 1323 most readily used normalization is that of flux control ratios and flux control factors (Gnaiger  
 1324 2014). Selection of the state of maximum flux in a protocol as the reference state has the  
 1325 advantages of: (1) internal normalization; (2) statistical linearization of the response in the range  
 1326 of 0 to 1; and (3) consideration of maximum flux for integrating a very large number of  
 1327 elemental steps in the OXPHOS- or ET-pathways. This reduces the risk of selecting a functional  
 1328 marker that is specifically altered by the treatment or pathology, yet increases the chance that  
 1329 the highly integrative pathway is disproportionately affected, *e.g.* the OXPHOS- rather than  
 1330 ET-pathway in case of an enzymatic defect in the phosphorylation-pathway. In this case,  
 1331 additional information can be obtained by reporting flux control ratios based on a reference  
 1332 state which indicates stable tissue-mass specific flux. Stereological determination of  
 1333 mitochondrial content via two-dimensional transmission electron microscopy can have  
 1334 limitations due to the dynamics of mitochondrial size (Meinild Lundby *et al.* 2017). Accurate  
 1335 determination of three-dimensional volume by two-dimensional microscopy can be both time  
 1336 consuming and statistically challenging (Larsen *et al.* 2012). Using mitochondrial marker  
 1337 enzymes (citrate synthase activity, Complex I–IV amount or activity) for normalization of flux  
 1338 is limited in part by the same factors that apply to the use of flux control ratios. Strong  
 1339 correlations between various mitochondrial markers and citrate synthase activity (Reichmann  
 1340 *et al.* 1985; Boushel *et al.* 2007; Mogensen *et al.* 2007) are expected in a specific tissue of  
 1341 healthy subjects and in disease states not specifically targeting citrate synthase. Citrate synthase  
 1342 activity is acutely modifiable by exercise (Tonkonogi *et al.* 1997; Leek *et al.* 2001). Evaluation  
 1343 of mitochondrial markers related to a selected age and sex cohort cannot be extrapolated to  
 1344 provide recommendations for normalization in respirometric diagnosis of disease, in different  
 1345 states of development and ageing, different cell types, tissues, and species. mtDNA normalised

1346 to nDNA via qPCR is correlated to functional mitochondrial markers including OXPHOS- and  
 1347 ET-capacity in some cases (Puntschart *et al.* 1995; Wang *et al.* 1999; Menshikova *et al.* 2006;  
 1348 Boushel *et al.* 2007), but lack of such correlations have been reported (Menshikova *et al.* 2005;  
 1349 Schultz and Wiesner 2000; Pesta *et al.* 2011). Several studies indicate a strong correlation  
 1350 between cardiolipin content and increase in mitochondrial functionality with exercise  
 1351 (Menshikova *et al.* 2005; Menshikova *et al.* 2007; Larsen *et al.* 2012; Faber *et al.* 2014), but its  
 1352 use as a general mitochondrial biomarker in disease remains questionable.  
 1353

#### 1354 4.5. Conversion: units and normalization

1355 Many different units have been used to report the rate of oxygen consumption, OCR  
 1356 (Table 8). SI base units provide the common reference for introducing the theoretical principles  
 1357 (Fig. 8), and are used with appropriately chosen SI prefixes to express numerical data in the  
 1358 most practical format, with an effort towards unification within specific areas of application  
 1359 (Table 9). For studies of cells, we recommend that respiration be expressed, as far as possible,  
 1360 as: (1) O<sub>2</sub> flux normalized for a mitochondrial marker, for separation of the effects of  
 1361 mitochondrial quality and content on cell respiration (this includes FCRs as a normalization for  
 1362 a functional mitochondrial marker); (2) O<sub>2</sub> flux in units of cell volume or mass, for comparison  
 1363 of respiration of cells with different cell size (Renner *et al.* 2003) and with studies on tissue  
 1364 preparations, and (3) O<sub>2</sub> flow in units of attomole (10<sup>-18</sup> mol) of O<sub>2</sub> consumed in a second by  
 1365 each cell [amol·s<sup>-1</sup>·cell<sup>-1</sup>], numerically equivalent to [pmol·s<sup>-1</sup>·10<sup>-6</sup> cells]. This convention  
 1366 allows information to be easily used when designing experiments in which oxygen consumption  
 1367 must be considered. For example, to estimate the volume-specific O<sub>2</sub> flux in an instrument  
 1368 chamber that would be expected at a particular cell number concentration, one simply needs to  
 1369 multiply the flow per cell by the number of cells per volume of interest. This provides the  
 1370 amount of O<sub>2</sub> [mol] consumed per time [s<sup>-1</sup>] per unit volume [L<sup>-1</sup>]. At an O<sub>2</sub> flow of 100  
 1371 amol·s<sup>-1</sup>·cell<sup>-1</sup> and a cell density of 10<sup>9</sup> cells·L<sup>-1</sup> (10<sup>6</sup> cells·mL<sup>-1</sup>), the volume-specific O<sub>2</sub> flux is  
 1372 100 nmol·s<sup>-1</sup>·L<sup>-1</sup> (100 pmol·s<sup>-1</sup>·mL<sup>-1</sup>).

1373 Although volume is expressed as m<sup>3</sup> using the SI base unit, the litre [dm<sup>3</sup>] is the basic unit  
 1374 of volume for concentration and is used for most solution chemical kinetics. If one multiplies  
 1375  $J_{\text{cell},\text{O}_2}$  by  $C_{\text{Ncell}}$ , then the result will not only be the amount of O<sub>2</sub> [mol] consumed per time [s<sup>-1</sup>]  
 1376 in one litre [L<sup>-1</sup>], but also the change in the concentration of oxygen per second (for any volume  
 1377 of an ideally closed system). This is ideal for kinetic modeling as it blends with chemical rate  
 1378 equations where concentrations are typically expressed in mol·L<sup>-1</sup> (Wagner *et al.* 2011). In  
 1379 studies of multinuclear cells, such as differentiated skeletal muscle cells, it is easy to determine  
 1380 the number of nuclei but not the total number of cells. A generalized concept, therefore, is  
 1381 obtained by substituting cells by nuclei as the sample entity. This does not hold, however, for  
 1382 enucleated platelets.  
 1383

#### 1384 4.6. Conversion: oxygen, proton and ATP flux

1386  $J_{\text{O}_2,\text{k}}$  is coupled in mitochondrial steady states to proton cycling,  $J_{\text{H}^+\infty} = J_{\text{H}^+,\text{pos}} = J_{\text{H}^+,\text{neg}}$   
 1387 (Fig. 2).  $J_{\text{H}^+,\text{pos}/\text{n}}$  and  $J_{\text{H}^+,\text{neg}/\text{n}}$  [nmol·s<sup>-1</sup>·L<sup>-1</sup>] are converted into electrical units,  $J_{\text{H}^+,\text{pos}/\text{e}}$  [mC·s<sup>-1</sup>·L<sup>-1</sup>  
 1388 = mA·L<sup>-1</sup>] =  $J_{\text{H}^+,\text{pos}/\text{n}}$  [nmol·s<sup>-1</sup>·L<sup>-1</sup>]· $F$  [C·mol<sup>-1</sup>]·10<sup>-6</sup> (Table 4). At a  $J_{\text{H}^+,\text{pos}}/J_{\text{O}_2,\text{k}}$  ratio or H<sup>+</sup><sub>pos</sub>/O<sub>2</sub>  
 1389 of 20 (H<sup>+</sup><sub>pos</sub>/O = 10), a volume-specific O<sub>2</sub> flux of 100 nmol·s<sup>-1</sup>·L<sup>-1</sup> would correspond to a proton  
 1390 flux of 2,000 nmol H<sup>+</sup><sub>pos</sub>·s<sup>-1</sup>·L<sup>-1</sup> or volume-specific current of 193 mA·L<sup>-1</sup>.

$$1391 J_{\text{V},\text{H}^+,\text{pos}/\text{e}} [\text{mA}\cdot\text{L}^{-1}] = J_{\text{V},\text{H}^+,\text{pos}/\text{n}} \cdot F \cdot 10^{-6} [\text{nmol}\cdot\text{s}^{-1}\cdot\text{L}^{-1}\cdot\text{mC}\cdot\text{nmol}^{-1}] \quad (\text{Eq. 5.1})$$

$$1392 J_{\text{V},\text{H}^+,\text{pos}/\text{e}} [\text{mA}\cdot\text{L}^{-1}] = J_{\text{V},\text{O}_2} \cdot (\text{H}^+_{\text{pos}}/\text{O}_2) \cdot F \cdot 10^{-6} [\text{mC}\cdot\text{s}^{-1}\cdot\text{L}^{-1} = \text{mA}\cdot\text{L}^{-1}] \quad (\text{Eq. 5.2})$$

1393 ET-capacity in various human cell types including HEK 293, primary HUVEC and fibroblasts  
 1394 ranges from 50 to 180 amol·s<sup>-1</sup>·cell<sup>-1</sup>, measured in intact cells in the noncoupled state (see  
 1395 Gnaiger 2014). At 100 amol·s<sup>-1</sup>·cell<sup>-1</sup> corrected for  $R_{\text{ox}}$  (corresponding to a catabolic power of  
 1396 -48 pW·cell<sup>-1</sup>), the current across the mt-membranes,  $I_e$ , approximates 193 pA·cell<sup>-1</sup> or 0.2 nA



1397 per cell. See Rich (2003) for an extension of quantitative bioenergetics from the molecular to  
 1398 the human scale, with a transmembrane proton flux equivalent to 520 A in an adult at a catabolic  
 1399 power of -110 W. Modelling approaches illustrate the link between protonmotive force and  
 1400 currents (Willis *et al.* 2016). For NADH- and succinate-linked respiration, the mechanistic  
 1401  $P_{\gg}/O_2$  ratio (referring to the full 4 electron reduction of  $O_2$ ) is calculated at  $20/3.7 = 5.4$  and  
 1402  $12/3.7 = 3.3$ , respectively (Eq. 6). The classical  $P_{\gg}/O$  ratios (referring to the 2 electron reduction  
 1403 of  $0.5 O_2$ ) are 2.7 and 1.6 (Watt *et al.* 2010), in direct agreement with the measured  $P_{\gg}/O$  ratio  
 1404 for succinate of  $1.58 \pm 0.02$  (Gnaiger *et al.* 2000; for detailed reviews see Wikström and  
 1405 Hummer 2012; Sazanov 2015),

$$1406 \quad P_{\gg}/O_2 = (H^+_{\text{pos}}/O_2)/(H^+_{\text{neg}}/P_{\gg}) \quad (\text{Eq. 6})$$

1407 In summary (Fig. 1),

$$1408 \quad J_{V,P_{\gg}} [\text{nmol}\cdot\text{s}^{-1}\cdot\text{L}^{-1}] = J_{V,O_2} \cdot (H^+_{\text{pos}}/O_2)/(H^+_{\text{neg}}/P_{\gg}) \quad (\text{Eq. 7.1})$$

$$1409 \quad J_{V,P_{\gg}} [\text{nmol}\cdot\text{s}^{-1}\cdot\text{L}^{-1}] = J_{V,O_2} \cdot (P_{\gg}/O_2) \quad (\text{Eq. 7.2})$$

1410 We consider isolated mitochondria as powerhouses and proton pumps as molecular  
 1411 machines to relate experimental results to energy metabolism of the intact cell. The cellular  
 1412  $P_{\gg}/O_2$  based on oxidation of glycogen is increased by the glycolytic (fermentative) substrate-  
 1413 level phosphorylation of 3  $P_{\gg}/\text{Glyc}$ , *i.e.*, 0.5 mol  $P_{\gg}$  for each mol  $O_2$  consumed in the complete  
 1414 oxidation of a mol glycosyl unit (Glyc). Adding 0.5 to the mitochondrial  $P_{\gg}/O_2$  ratio of 5.4  
 1415 yields a bioenergetic cell physiological  $P_{\gg}/O_2$  ratio close to 6. Two NADH equivalents are  
 1416 formed during glycolysis and transported from the cytosol into the mitochondrial matrix, either  
 1417 by the malate-aspartate shuttle or by the glycerophosphate shuttle resulting in different  
 1418 theoretical yield of ATP generated by mitochondria, the energetic cost of which potentially  
 1419 must be taken into account. Considering also substrate-level phosphorylation in the TCA cycle,  
 1420 this high  $P_{\gg}/O_2$  ratio not only reflects proton translocation and OXPHOS studied in isolation,  
 1421 but integrates mitochondrial physiology with energy transformation in the living cell (Gnaiger  
 1422 1993a).

1423  
 1424 **Table 8. Conversion of various units used in respirometry and**  
 1425 **ergometry.** e is the number of electrons or reducing equivalents.  $z_B$  is the  
 1426 charge number of entity B.  
 1427

1 Unit	x	Multiplication factor	SI-Unit	Note
ng.atom $O\cdot s^{-1}$	(2 e)	0.5	nmol $O_2\cdot s^{-1}$	
ng.atom $O\cdot \text{min}^{-1}$	(2 e)	8.33	pmol $O_2\cdot s^{-1}$	
natom $O\cdot \text{min}^{-1}$	(2 e)	8.33	pmol $O_2\cdot s^{-1}$	
nmol $O_2\cdot \text{min}^{-1}$	(4 e)	16.67	pmol $O_2\cdot s^{-1}$	
nmol $O_2\cdot h^{-1}$	(4 e)	0.2778	pmol $O_2\cdot s^{-1}$	
mL $O_2\cdot \text{min}^{-1}$ at STPD <sup>a</sup>		0.744	$\mu\text{mol } O_2\cdot s^{-1}$	1
W = J/s at -470 kJ/mol $O_2$		-2.128	$\mu\text{mol } O_2\cdot s^{-1}$	
mA = mC $\cdot s^{-1}$	( $z_{H^+} = 1$ )	10.36	nmol $H^+\cdot s^{-1}$	2
mA = mC $\cdot s^{-1}$	( $z_{O_2} = 4$ )	2.59	nmol $O_2\cdot s^{-1}$	2
nmol $H^+\cdot s^{-1}$	( $z_{H^+} = 1$ )	0.09649	mA	3
nmol $O_2\cdot s^{-1}$	( $z_{O_2} = 4$ )	0.38594	mA	3

1428 1 At standard temperature and pressure dry (STPD: 0 °C = 273.15 K and 1 atm =  
 1429 101.325 kPa = 760 mmHg), the molar volume of an ideal gas,  $V_m$ , and  $V_{m,O_2}$  is  
 1430 22.414 and 22.392 L $\cdot\text{mol}^{-1}$  respectively. Rounded to three decimal places, both  
 1431 values yield the conversion factor of 0.744. For comparison at NTPD (20 °C),  
 1432  $V_{m,O_2}$  is 24.038 L $\cdot\text{mol}^{-1}$ . Note that the SI standard pressure is 100 kPa.

1433 2 The multiplication factor is  $10^6/(z_B\cdot F)$ .

1434 3 The multiplication factor is  $z_B \cdot F/10^6$ .

1435

1436

**Table 9. Conversion of units with preservation of numerical values.**

Name	Frequently used unit	Equivalent unit	Note
Volume-specific flux, $J_{V,O_2}$	$\text{pmol} \cdot \text{s}^{-1} \cdot \text{mL}^{-1}$ $\text{mmol} \cdot \text{s}^{-1} \cdot \text{L}^{-1}$	$\text{nmol} \cdot \text{s}^{-1} \cdot \text{L}^{-1}$ $\text{mol} \cdot \text{s}^{-1} \cdot \text{m}^{-3}$	1
Cell-specific flow, $I_{O_2}$	$\text{pmol} \cdot \text{s}^{-1} \cdot 10^{-6}$ cells $\text{pmol} \cdot \text{s}^{-1} \cdot 10^{-9}$ cells	$\text{amol} \cdot \text{s}^{-1} \cdot \text{cell}^{-1}$ $\text{zmol} \cdot \text{s}^{-1} \cdot \text{cell}^{-1}$	2 3
Cell number concentration, $C_{Nce}$	$10^6$ cells $\cdot \text{mL}^{-1}$	$10^9$ cells $\cdot \text{L}^{-1}$	
Mitochondrial protein concentration, $C_{mte}$	$0.1 \text{ mg} \cdot \text{mL}^{-1}$	$0.1 \text{ g} \cdot \text{L}^{-1}$	
Mass-specific flux, $J_{m,O_2}$	$\text{pmol} \cdot \text{s}^{-1} \cdot \text{mg}^{-1}$	$\text{nmol} \cdot \text{s}^{-1} \cdot \text{g}^{-1}$	4
Catabolic power, $P_{O_2,k}$	$\mu\text{W} \cdot 10^{-6}$ cells	$\text{pW} \cdot \text{cell}^{-1}$	1
Volume	1,000 L L mL $\mu\text{L}$ fL	$\text{m}^3$ (1,000 kg) $\text{dm}^3$ (kg) $\text{cm}^3$ (g) $\text{mm}^3$ (mg) $\mu\text{m}^3$ (pg)	5
Amount of substance concentration	$\text{M} = \text{mol} \cdot \text{L}^{-1}$	$\text{mol} \cdot \text{dm}^{-3}$	

1437

1438

1439

1440

1441

1442

1443

1444

1445

1446

1447

1448

1449

1450

1451

## 5. Conclusions

MitoEAGLE can serve as a gateway to better diagnose mitochondrial respiratory defects linked to genetic variation, age-related health risks, sex-specific mitochondrial performance, lifestyle with its effects on degenerative diseases, and thermal and chemical environment. The present recommendations on coupling control states and rates, linked to the concept of the protonmotive force, are limited to studies with mitochondrial preparations. These will be extended in a series of reports on pathway control of mitochondrial respiration, respiratory states in intact cells, and harmonization of experimental procedures.

1452

### Box 5: Mitochondrial and cell respiration

1453

1454

1455

1456

1457

1458

1459

1460

1461

1462

1463

Mitochondrial and cell respiration is the process of highly exergonic and exothermic energy transformation in which scalar redox reactions are coupled to vectorial ion translocation across a semipermeable membrane, which separates the small volume of a bacterial cell or mitochondrion from the larger volume of its surroundings. The electrochemical exergy can be partially conserved in the phosphorylation of ADP to ATP or in ion pumping, or dissipated in an electrochemical short-circuit. Respiration is thus clearly distinguished from fermentation as the counterpart of cellular core energy metabolism. Respiration is separated in mitochondrial preparations from the partial contribution of fermentative pathways of the intact cell. According to this definition, residual oxygen consumption, as measured after inhibition of mitochondrial electron transfer, does not belong to the class of catabolic reactions and is, therefore, subtracted from total oxygen consumption to obtain baseline-corrected respiration.

1464

1465

1466

1467

The optimal choice for expressing mitochondrial and cell respiration (**Box 5**) as  $\text{O}_2$  flow per biological system, and normalization for specific tissue-markers (volume, mass, protein) and mitochondrial markers (volume, protein, content, mtDNA, activity of marker enzymes,

1468 respiratory reference state) is guided by the scientific question under study. Interpretation of  
 1469 the obtained data depends critically on appropriate normalization, and therefore reporting rates  
 1470 merely as  $\text{nmol}\cdot\text{s}^{-1}$  is discouraged, since it restricts the analysis to intra-experimental  
 1471 comparison of relative (qualitative) differences. Expressing  $\text{O}_2$  consumption per cell may not  
 1472 be possible when dealing with tissues. For studies with mitochondrial preparations, we  
 1473 recommend that normalizations be provided as far as possible: (1) on a per cell basis as  $\text{O}_2$  flow  
 1474 (a biophysical normalization); (2) per g cell or tissue protein, or per cell or tissue mass as mass-  
 1475 specific  $\text{O}_2$  flux (a cellular normalization); and (3) per mitochondrial marker as mt-specific flux  
 1476 (a mitochondrial normalization). With information on cell size and the use of multiple  
 1477 normalizations, maximum potential information is available (Renner *et al.* 2003; Wagner *et al.*  
 1478 2011; Gnaiger 2014). When using isolated mitochondria, mitochondrial protein is a frequently  
 1479 applied mitochondrial marker, the use of which is basically restricted to isolated mitochondria.  
 1480 Mitochondrial markers, such as citrate synthase activity as an enzymatic matrix marker, provide  
 1481 a link to the tissue of origin on the basis of calculating the mitochondrial yield, *i.e.*, the fraction  
 1482 of mitochondrial marker obtained from a unit mass of tissue.

### 1484 **Acknowledgements**

1485 We thank M. Beno for management assistance. Supported by COST Action CA15203  
 1486 MitoEAGLE and K-Regio project MitoFit (EG).

1487  
 1488 **Competing financial interests:** E.G. is founder and CEO of Oroboros Instruments, Innsbruck,  
 1489 Austria.

### 1491 **6. References**

- 1492 Altmann R (1894) Die Elementarorganismen und ihre Beziehungen zu den Zellen. Zweite vermehrte Auflage.  
 1493 Verlag Von Veit & Comp, Leipzig:160 pp.
- 1494 Beard DA (2005) A biophysical model of the mitochondrial respiratory system and oxidative phosphorylation.  
 1495 PLoS Comput Biol 1(4):e36.
- 1496 Benda C (1898) Über die Spermatogenese der Vertebraten und höherer Evertebraten II Theil: Die Histogenese  
 1497 der Spermien. Arch Anat Physiol 73:393-8.
- 1498 Birkedal R, Laasmaa M, Vendelin M (2014) The location of energetic compartments affects energetic  
 1499 communication in cardiomyocytes. Front Physiol 5:376. doi: 10.3389/fphys.2014.00376. eCollection 2014.
- 1500 Breton S, Beaupré HD, Stewart DT, Hoeh WR, Blier PU (2007) The unusual system of doubly uniparental  
 1501 inheritance of mtDNA: isn't one enough? Trends Genet 23:465-74.
- 1502 Brown GC (1992) Control of respiration and ATP synthesis in mammalian mitochondria and cells. Biochem J  
 1503 284:1-13.
- 1504 Campos JC, Queliconi BB, Bozi LHM, Bechara LRG, Dourado PMM, Andres AM, Jannig PR, Gomes KMS,  
 1505 Zambelli VO, Rocha-Resende C, Guatimosim S, Brum PC, Mochly-Rosen D, Gottlieb RA, Kowaltowski AJ,  
 1506 Ferreira JCB (2017) Exercise reestablishes autophagic flux and mitochondrial quality control in heart failure.  
 1507 Autophagy 13:310-317.
- 1508 Chance B, Williams GR (1955a) Respiratory enzymes in oxidative phosphorylation. I. Kinetics of oxygen  
 1509 utilization. J Biol Chem 217:383-93.
- 1510 Chance B, Williams GR (1955b) Respiratory enzymes in oxidative phosphorylation: III. The steady state. J Biol  
 1511 Chem 217:409-27.
- 1512 Chance B, Williams GR (1955c) Respiratory enzymes in oxidative phosphorylation. IV. The respiratory chain. J  
 1513 Biol Chem 217:429-38.
- 1514 Chance B, Williams GR (1956) The respiratory chain and oxidative phosphorylation. Adv Enzymol Relat Subj  
 1515 Biochem 17:65-134.
- 1516 Cobb LJ, Lee C, Xiao J, Yen K, Wong RG, Nakamura HK, Mehta HH, Gao Q, Ashur C, Huffman DM, Wan J,  
 1517 Muzumdar R, Barzilai N, Cohen P (2016) Naturally occurring mitochondrial-derived peptides are age-  
 1518 dependent regulators of apoptosis, insulin sensitivity, and inflammatory markers. Aging (Albany NY) 8:796-  
 1519 809.
- 1520 Cohen ER, Cvitas T, Frey JG, Holmström B, Kuchitsu K, Marquardt R, Mills I, Pavese F, Quack M, Stohner J,  
 1521 Strauss HL, Takami M, Thor HL (2008) Quantities, units and symbols in physical chemistry, IUPAC Green  
 1522 Book, 3rd Edition, 2nd Printing, IUPAC & RSC Publishing, Cambridge.
- 1523 Cooper H, Hedges LV, Valentine JC, eds (2009) The handbook of research synthesis and meta-analysis. Russell  
 1524 Sage Foundation.

- 1525 Coopersmith J (2010) Energy, the subtle concept. The discovery of Feynman's blocks from Leibnitz to Einstein.  
1526 Oxford University Press:400 pp.
- 1527 Cummins J (1998) Mitochondrial DNA in mammalian reproduction. *Rev Reprod* 3:172–82.
- 1528 Dai Q, Shah AA, Garde RV, Yonish BA, Zhang L, Medvitz NA, Miller SE, Hansen EL, Dunn CN, Price TM  
1529 (2013) A truncated progesterone receptor (PR-M) localizes to the mitochondrion and controls cellular  
1530 respiration. *Mol Endocrinol* 27:741-53.
- 1531 Divakaruni AS, Brand MD (2011) The regulation and physiology of mitochondrial proton leak. *Physiology*  
1532 (Bethesda) 26:192-205.
- 1533 Doerrier C, Garcia-Souza LF, Krumschnabel G, Wohlfarter Y, Mészáros AT, Gnaiger E (2017) High-Resolution  
1534 FluoRespirometry and OXPHOS protocols for human cells, permeabilized fibres from small biopsies of  
1535 muscle and isolated mitochondria. *Methods Mol. Biol.* (in press)
- 1536 Doskey CM, van 't Erve TJ, Wagner BA, Buettner GR (2015) Moles of a substance per cell is a highly  
1537 informative dosing metric in cell culture. *PLOS ONE* 10:e0132572.
- 1538 Drahota Z, Milerová M, Stieglerová A, Houstek J, Ostádal B (2004) Developmental changes of cytochrome *c*  
1539 oxidase and citrate synthase in rat heart homogenate. *Physiol Res* 53:119-22.
- 1540 Duarte FV, Palmeira CM, Rolo AP (2014) The role of microRNAs in mitochondria: small players acting wide.  
1541 *Genes (Basel)* 5:865-86.
- 1542 Dufour S, Rousse N, Canioni P, Diolez P (1996) Top-down control analysis of temperature effect on oxidative  
1543 phosphorylation. *Biochem J* 314:743-51.
- 1544 Ernster L, Schatz G (1981) Mitochondria: a historical review. *J Cell Biol* 91:227s-55s.
- 1545 Estabrook RW (1967) Mitochondrial respiratory control and the polarographic measurement of ADP:O ratios.  
1546 *Methods Enzymol* 10:41-7.
- 1547 Faber C, Zhu ZJ, Castellino S, Wagner DS, Brown RH, Peterson RA, Gates L, Barton J, Bickett M, Hagerty L,  
1548 Kimbrough C, Sola M, Bailey D, Jordan H, Elangbam CS (2014) Cardiolipin profiles as a potential  
1549 biomarker of mitochondrial health in diet-induced obese mice subjected to exercise, diet-restriction and  
1550 ephedrine treatment. *J Appl Toxicol* 34:1122-9.
- 1551 Fell D (1997) Understanding the control of metabolism. Portland Press.
- 1552 Garlid KD, Beavis AD, Ratkje SK (1989) On the nature of ion leaks in energy-transducing membranes. *Biochim*  
1553 *Biophys Acta* 976:109-20.
- 1554 Garlid KD, Semrad C, Zinchenko V. Does redox slip contribute significantly to mitochondrial respiration? In:  
1555 Schuster S, Rigoulet M, Ouhabi R, Mazat J-P, eds (1993) Modern trends in biothermokinetics. Plenum Press,  
1556 New York, London:287-93.
- 1557 Gerö D, Szabo C (2016) Glucocorticoids suppress mitochondrial oxidant production via upregulation of  
1558 uncoupling protein 2 in hyperglycemic endothelial cells. *PLoS One* 11:e0154813.
- 1559 Gibney E (2017) New definitions of scientific units are on the horizon. *Nature* 550:312–13.
- 1560 Gnaiger E. Efficiency and power strategies under hypoxia. Is low efficiency at high glycolytic ATP production a  
1561 paradox? In: Surviving Hypoxia: Mechanisms of Control and Adaptation. Hochachka PW, Lutz PL, Sick T,  
1562 Rosenthal M, Van den Thillart G, eds (1993a) CRC Press, Boca Raton, Ann Arbor, London, Tokyo:77-109.
- 1563 Gnaiger E (1993b) Nonequilibrium thermodynamics of energy transformations. *Pure Appl Chem* 65:1983-2002.
- 1564 Gnaiger E (2001) Bioenergetics at low oxygen: dependence of respiration and phosphorylation on oxygen and  
1565 adenosine diphosphate supply. *Respir Physiol* 128:277-97.
- 1566 Gnaiger E (2009) Capacity of oxidative phosphorylation in human skeletal muscle. New perspectives of  
1567 mitochondrial physiology. *Int J Biochem Cell Biol* 41:1837-45.
- 1568 Gnaiger E (2014) Mitochondrial pathways and respiratory control. An introduction to OXPHOS analysis. 4th ed.  
1569 *Mitochondr Physiol Network* 19.12. Oroboros MiPNet Publications, Innsbruck:80 pp.
- 1570 Gnaiger E, Méndez G, Hand SC (2000) High phosphorylation efficiency and depression of uncoupled respiration  
1571 in mitochondria under hypoxia. *Proc Natl Acad Sci USA* 97:11080-5.
- 1572 Greggio C, Jha P, Kulkarni SS, Lagarrigue S, Broskey NT, Boutant M, Wang X, Conde Alonso S, Ofori E,  
1573 Auwerx J, Cantó C, Amati F (2017) Enhanced respiratory chain supercomplex formation in response to  
1574 exercise in human skeletal muscle. *Cell Metab* 25:301-11.
- 1575 Hofstadter DR (1979) Gödel, Escher, Bach: An eternal golden braid. A metaphorical fugue on minds and  
1576 machines in the spirit of Lewis Carroll. Harvester Press:499 pp.
- 1577 Illaste A, Laasmaa M, Peterson P, Vendelin M (2012) Analysis of molecular movement reveals latticelike  
1578 obstructions to diffusion in heart muscle cells. *Biophys J* 102:739-48.
- 1579 Jasienski M, Bazzaz FA (1999) The fallacy of ratios and the testability of models in biology. *Oikos* 84:321-26.
- 1580 Jepihhina N, Beraud N, Sepp M, Birkedal R, Vendelin M (2011) Permeabilized rat cardiomyocyte response  
1581 demonstrates intracellular origin of diffusion obstacles. *Biophys J* 101:2112-21.
- 1582 Klepinin A, Ounpuu L, Guzun R, Chekulayev V, Timohhina N, Tepp K, Shevchuk I, Schlattner U, Kaambre T  
1583 (2016) Simple oxygraphic analysis for the presence of adenylate kinase 1 and 2 in normal and tumor cells. *J*  
1584 *Bioenerg Biomembr* 48:531-48.
- 1585 Klingenberg M (2017) UCP1 - A sophisticated energy valve. *Biochimie* 134:19-27.

- 1586 Koit A, Shevchuk I, Ounpuu L, Klepinin A, Chekulayev V, Timohhina N, Tepp K, Puurand M, Truu L, Heck K,  
 1587 Valvere V, Guzun R, Kaambre T (2017) Mitochondrial respiration in human colorectal and breast cancer  
 1588 clinical material is regulated differently. *Oxid Med Cell Longev* 1372640.
- 1589 Komlódi T, Tretter L (2017) Methylene blue stimulates substrate-level phosphorylation catalysed by succinyl-  
 1590 CoA ligase in the citric acid cycle. *Neuropharmacology* 123:287-98.
- 1591 Lane N (2005) *Power, sex, suicide: mitochondria and the meaning of life*. Oxford University Press:354 pp.
- 1592 Larsen S, Nielsen J, Neigaard Nielsen C, Nielsen LB, Wibrand F, Stride N, Schroder HD, Boushel RC, Helge  
 1593 JW, Dela F, Hey-Mogensen M (2012) Biomarkers of mitochondrial content in skeletal muscle of healthy  
 1594 young human subjects. *J Physiol* 590:3349-60.
- 1595 Lee C, Zeng J, Drew BG, Sallam T, Martin-Montalvo A, Wan J, Kim SJ, Mehta H, Hevener AL, de Cabo R,  
 1596 Cohen P (2015) The mitochondrial-derived peptide MOTS-c promotes metabolic homeostasis and reduces  
 1597 obesity and insulin resistance. *Cell Metab* 21:443-54.
- 1598 Lee SR, Kim HK, Song IS, Youm J, Dizon LA, Jeong SH, Ko TH, Heo HJ, Ko KS, Rhee BD, Kim N, Han J  
 1599 (2013) Glucocorticoids and their receptors: insights into specific roles in mitochondria. *Prog Biophys Mol*  
 1600 *Biol* 112:44-54.
- 1601 Leek BT, Mudaliar SR, Henry R, Mathieu-Costello O, Richardson RS (2001) Effect of acute exercise on citrate  
 1602 synthase activity in untrained and trained human skeletal muscle. *Am J Physiol Regul Integr Comp Physiol*  
 1603 280:R441-7.
- 1604 Lemieux H, Blier PU, Gnaiger E (2017) Remodeling pathway control of mitochondrial respiratory capacity by  
 1605 temperature in mouse heart: electron flow through the Q-junction in permeabilized fibers. *Sci Rep* 7:2840.
- 1606 Lenaz G, Tioli G, Falasca AI, Genova ML (2017) Respiratory supercomplexes in mitochondria. In: *Mechanisms*  
 1607 *of primary energy trasduction in biology*. M Wikstrom (ed) Royal Society of Chemistry Publishing, London,  
 1608 UK:296-337.
- 1609 Margulis L (1970) *Origin of eukaryotic cells*. New Haven: Yale University Press.
- 1610 Meinild Lundby AK, Jacobs RA, Gehrig S, de Leur J, Hauser M, Bonne TC, Flück D, Dandanell S, Kirk N,  
 1611 Kaech A, Ziegler U, Larsen S, Lundby C (2017) Exercise training increases skeletal muscle mitochondrial  
 1612 volume density by enlargement of existing mitochondria and not de novo biogenesis. *Acta Physiol (Oxf)*  
 1613 [Epub ahead of print].
- 1614 Menshikova EV, Ritov VB, Fairfull L, Ferrell RE, Kelley DE, Goodpaster BH (2006) Effects of exercise on  
 1615 mitochondrial content and function in aging human skeletal muscle. *J Gerontol A Biol Sci Med Sci* 61:534-  
 1616 40.
- 1617 Menshikova EV, Ritov VB, Ferrell RE, Azuma K, Goodpaster BH, Kelley DE (2007) Characteristics of skeletal  
 1618 muscle mitochondrial biogenesis induced by moderate-intensity exercise and weight loss in obesity. *J Appl*  
 1619 *Physiol* (1985) 103:21-7.
- 1620 Menshikova EV, Ritov VB, Toledo FG, Ferrell RE, Goodpaster BH, Kelley DE (2005) Effects of weight loss  
 1621 and physical activity on skeletal muscle mitochondrial function in obesity. *Am J Physiol Endocrinol Metab*  
 1622 288:E818-25.
- 1623 Miller GA (1991) *The science of words*. Scientific American Library New York:276 pp. Mitchell P (1961)  
 1624 Coupling of phosphorylation to electron and hydrogen transfer by a chemi-osmotic type of mechanism.  
 1625 *Nature* 191:144-8.
- 1626 Mitchell P (2011) Chemiosmotic coupling in oxidative and photosynthetic phosphorylation. *Biochim Biophys*  
 1627 *Acta Bioenergetics* 1807:1507-38.
- 1628 Mitchell P, Moyle J (1967) Respiration-driven proton translocation in rat liver mitochondria. *Biochem J*  
 1629 105:1147-62.
- 1630 Mogensen M, Sahlin K, Fernström M, Glintborg D, Vind BF, Beck-Nielsen H, Højlund K (2007) Mitochondrial  
 1631 respiration is decreased in skeletal muscle of patients with type 2 diabetes. *Diabetes* 56:1592-9.
- 1632 Moreno M, Giacco A, Di Munno C, Goglia F (2017) Direct and rapid effects of 3,5-diiodo-L-thyronine (T2).  
 1633 *Mol Cell Endocrinol* 7207:30092-8.
- 1634 Morrow RM, Picard M, Derbeneva O, Leipzig J, McManus MJ, Gousspillou G, Barbat-Artigas S, Dos Santos C,  
 1635 Hepple RT, Murdock DG, Wallace DC (2017) Mitochondrial energy deficiency leads to hyperproliferation of  
 1636 skeletal muscle mitochondria and enhanced insulin sensitivity. *Proc Natl Acad Sci U S A* 114:2705-10.
- 1637 Paradies G, Paradies V, De Benedictis V, Ruggiero FM, Petrosillo G (2014) Functional role of cardiolipin in  
 1638 mitochondrial bioenergetics. *Biochim Biophys Acta* 1837:408-17.
- 1639 Pesta D, Hoppel F, Macek C, Messner H, Faulhaber M, Kobel C, Parson W, Burtcher M, Schocke M, Gnaiger  
 1640 E (2011) Similar qualitative and quantitative changes of mitochondrial respiration following strength and  
 1641 endurance training in normoxia and hypoxia in sedentary humans. *Am J Physiol Regul Integr Comp Physiol*  
 1642 301:R1078-87.
- 1643 Price TM, Dai Q (2015) The role of a mitochondrial progesterone receptor (PR-M) in progesterone action.  
 1644 *Semin Reprod Med* 33:185-94.
- 1645 Prigogine I (1967) *Introduction to thermodynamics of irreversible processes*. Interscience, New York, 3rd  
 1646 ed:147pp.

- 1647 Puchowicz MA, Varnes ME, Cohen BH, Friedman NR, Kerr DS, Hoppel CL (2004) Oxidative phosphorylation  
 1648 analysis: assessing the integrated functional activity of human skeletal muscle mitochondria – case studies.  
 1649 *Mitochondrion* 4:377-85. Puntschart A, Claassen H, Jostardt K, Hoppeler H, Billeter R (1995) mRNAs of  
 1650 enzymes involved in energy metabolism and mtDNA are increased in endurance-trained athletes. *Am J*  
 1651 *Physiol* 269:C619-25.
- 1652 Quiros PM, Mottis A, Auwerx J (2016) Mitonuclear communication in homeostasis and stress. *Nat Rev Mol*  
 1653 *Cell Biol* 17:213-26.
- 1654 Reichmann H, Hoppeler H, Mathieu-Costello O, von Bergen F, Pette D (1985) Biochemical and ultrastructural  
 1655 changes of skeletal muscle mitochondria after chronic electrical stimulation in rabbits. *Pflugers Arch* 404:1-  
 1656 9.
- 1657 Renner K, Amberger A, Konwalinka G, Gnaiger E (2003) Changes of mitochondrial respiration, mitochondrial  
 1658 content and cell size after induction of apoptosis in leukemia cells. *Biochim Biophys Acta* 1642:115-23.
- 1659 Rich P (2003) Chemiosmotic coupling: The cost of living. *Nature* 421:583.
- 1660 Rostovtseva TK, Sheldon KL, Hassanzadeh E, Monge C, Saks V, Bezrukov SM, Sackett DL (2008) Tubulin  
 1661 binding blocks mitochondrial voltage-dependent anion channel and regulates respiration. *Proc Natl Acad Sci*  
 1662 *USA* 105:18746-51.
- 1663 Rustin P, Parfait B, Chretien D, Bourgeron T, Djouadi F, Bastin J, Rötig A, Munnich A (1996) Fluxes of  
 1664 nicotinamide adenine dinucleotides through mitochondrial membranes in human cultured cells. *J Biol Chem*  
 1665 271:14785-90.
- 1666 Saks VA, Veksler VI, Kuznetsov AV, Kay L, Sikk P, Tiivel T, Tranqui L, Olivares J, Winkler K, Wiedemann F,  
 1667 Kunz WS (1998) Permeabilised cell and skinned fiber techniques in studies of mitochondrial function in  
 1668 vivo. *Mol Cell Biochem* 184:81-100.
- 1669 Salabei JK, Gibb AA, Hill BG (2014) Comprehensive measurement of respiratory activity in permeabilized cells  
 1670 using extracellular flux analysis. *Nat Protoc* 9:421-38.
- 1671 Sazanov LA (2015) A giant molecular proton pump: structure and mechanism of respiratory complex I. *Nat Rev*  
 1672 *Mol Cell Biol* 16:375-88.
- 1673 Schneider TD (2006) Claude Shannon: biologist. The founder of information theory used biology to formulate  
 1674 the channel capacity. *IEEE Eng Med Biol Mag* 25:30-3.
- 1675 Schönfeld P, Dymkowska D, Wojtczak L (2009) Acyl-CoA-induced generation of reactive oxygen species in  
 1676 mitochondrial preparations is due to the presence of peroxisomes. *Free Radic Biol Med* 47:503-9.
- 1677 Schrödinger E (1944) What is life? The physical aspect of the living cell. Cambridge Univ Press.
- 1678 Schultz J, Wiesner RJ (2000) Proliferation of mitochondria in chronically stimulated rabbit skeletal muscle--  
 1679 transcription of mitochondrial genes and copy number of mitochondrial DNA. *J Bioenerg Biomembr* 32:627-  
 1680 34.
- 1681 Simson P, Jepihhina N, Laasmaa M, Peterson P, Birkedal R, Vendelin M (2016) Restricted ADP movement in  
 1682 cardiomyocytes: Cytosolic diffusion obstacles are complemented with a small number of open mitochondrial  
 1683 voltage-dependent anion channels. *J Mol Cell Cardiol* 97:197-203.
- 1684 Stucki JW, Ineichen EA (1974) Energy dissipation by calcium recycling and the efficiency of calcium transport  
 1685 in rat-liver mitochondria. *Eur J Biochem* 48:365-75.
- 1686 Tonkonogi M, Harris B, Sahlin K (1997) Increased activity of citrate synthase in human skeletal muscle after a  
 1687 single bout of prolonged exercise. *Acta Physiol Scand* 161:435-6.
- 1688 Waczulikova I, Habodaszova D, Cagalinec M, Ferko M, Ulicna O, Mateasik A, Sikurova L, Ziegelhöffer A  
 1689 (2007) Mitochondrial membrane fluidity, potential, and calcium transients in the myocardium from acute  
 1690 diabetic rats. *Can J Physiol Pharmacol* 85:372-81.
- 1691 Wagner BA, Venkataraman S, Buettner GR (2011) The rate of oxygen utilization by cells. *Free Radic Biol Med*  
 1692 51:700-712.
- 1693 Wang H, Hiatt WR, Barstow TJ, Brass EP (1999) Relationships between muscle mitochondrial DNA content,  
 1694 mitochondrial enzyme activity and oxidative capacity in man: alterations with disease. *Eur J Appl Physiol*  
 1695 *Occup Physiol* 80:22-7.
- 1696 Wang T (2010) Coulomb force as an entropic force. *Phys Rev D* 81:104045.
- 1697 Watt IN, Montgomery MG, Runswick MJ, Leslie AG, Walker JE (2010) Bioenergetic cost of making an  
 1698 adenosine triphosphate molecule in animal mitochondria. *Proc Natl Acad Sci U S A* 107:16823-7.
- 1699 Weibel ER, Hoppeler H (2005) Exercise-induced maximal metabolic rate scales with muscle aerobic capacity. *J*  
 1700 *Exp Biol* 208:1635-44.
- 1701 White DJ, Wolff JN, Pierson M, Gemmell NJ (2008) Revealing the hidden complexities of mtDNA inheritance.  
 1702 *Mol Ecol* 17:4925-42.
- 1703 Wikström M, Hummer G (2012) Stoichiometry of proton translocation by respiratory complex I and its  
 1704 mechanistic implications. *Proc Natl Acad Sci U S A* 109:4431-6.
- 1705 Willis WT, Jackman MR, Messer JI, Kuzmiak-Glancy S, Glancy B (2016) A simple hydraulic analog model of  
 1706 oxidative phosphorylation. *Med Sci Sports Exerc* 48:990-1000.